



Contents lists available at ScienceDirect

Lithos

journal homepage: [www.elsevier.com/locate/lithos](http://www.elsevier.com/locate/lithos)

## Neoproterozoic–middle Paleozoic tectono-magmatic evolution of the Gorny Altai terrane, northwest of the Central Asian Orogenic Belt: Constraints from detrital zircon U–Pb and Hf-isotope studies

Ming Chen <sup>a,b</sup>, Min Sun <sup>a,b,\*</sup>, Mikhail M. Buslov <sup>c,d</sup>, Keda Cai <sup>e</sup>, Guochun Zhao <sup>a</sup>, Jianping Zheng <sup>f</sup>, Elena S. Rubanova <sup>c</sup>, Elena E. Voytishchik <sup>d</sup>

<sup>a</sup> Department of Earth Sciences, The University of Hong Kong, Pokfulam Road, Hong Kong, China

<sup>b</sup> HKU Shenzhen Institute of Research and Innovation, Shenzhen, China

<sup>c</sup> Institute of Geology and Mineralogy, Siberian Branch, Russian Academy of Sciences, Novosibirsk 630090, Russia

<sup>d</sup> The Novosibirsk State University, Pirogova Street 2, Novosibirsk 630090, Russia

<sup>e</sup> Xinjiang Research Center for Mineral Resources, Xinjiang Institute of Ecology and Geography, Chinese Academy of Sciences, Urumqi 830011, China

<sup>f</sup> State Key Laboratory of Geological Processes and Mineral Resources, China University of Geosciences, Wuhan 430074, China

### ARTICLE INFO

#### Article history:

Received 18 October 2014

Accepted 24 March 2015

Available online xxx

#### Keywords:

Gorny Altai terrane

Kuznetsk–Altai island arc

Detrital zircons

Crustal evolution

### ABSTRACT

The Gorny Altai terrane (GA) is a key area in understanding the crustal evolution of the Central Asian Orogenic Belt (CAOB). This paper reports U–Pb and Hf-isotope data for detrital zircons from Cambrian to early Devonian sedimentary sequences to constrain their provenance, as well as the tectono-magmatic events and crustal growth in this region. Nearly all the detrital zircons are characterized by euhedral to subhedral morphology, high Th/U ratios (ca. 0.1–1.6) and typical oscillatory zoning, indicating a magmatic origin. The three samples from the Gorny Altai Group (middle Cambrian to early Ordovician) yield detrital zircon populations that are composed predominantly of 530–464 Ma grains, followed by a subordinate group of 641–549 Ma old. The Silurian and Devonian samples exhibit similar major zircon populations (555–456 Ma and 525–463 Ma, respectively), but a significant amount of additional 2431–772 Ma zircons occur in the early Devonian sample. Our results suggest that detritus from the nearby Kuznetsk–Altai intra-oceanic island arc served as a unitary source for the Cambrian–Silurian sedimentary sequences, but older detritus from other sources added to the early Devonian sequence. The low abundance of ca. 640–540 Ma detrital zircons may testify that this island arc was under a primitive stage in this period, when mafic volcanic rocks probably dominated. In contrast, the dominant population of ca. 530–470 Ma zircons may indicate an increased amount of granitic rocks in the source area, suggesting that the Kuznetsk–Altai island arc possibly evolved into a mature one in the Cambrian to early Ordovician. The ca. 530–470 Ma detrital zircons are almost exclusively featured by positive  $\varepsilon_{\text{Hf}}(t)$  values and have two-stage Hf model ages of ca. 1.40–0.45 Ga, indicating that the precursor magmas were sourced predominantly from heterogeneous juvenile materials. We conclude that the late Neoproterozoic to early Paleozoic magmatism in the Kuznetsk–Altai arc made a significant contribution to the crustal growth in the CAOB.

The absence of middle Ordovician to early Devonian detrital zircons possibly implies that the area changed to a passive margin in the middle Ordovician. Of special significance are the 2431–772 Ma zircons in the early Devonian sample, which are quite comparable to the Precambrian detrital zircons from the Altai–Mongolian terrane (AM) but distinct from those from the Siberian continent. This indicates that the AM is a plausible source for the 2431–772 Ma zircons. Our data therefore imply that the GA possibly amalgamated with the AM before the early Devonian rather than in the late Devonian to early Carboniferous as previously suggested.

© 2015 Elsevier B.V. All rights reserved.

### 1. Introduction

The Central Asian Orogenic Belt (CAOB), or named as the Altaids, is one of the largest Phanerozoic accretionary collages in the world

(e.g. Jahn, 2004; Sengör et al., 1993; Wilhem et al., 2012; Windley et al., 2007; Xiao et al., 2010). It covers a huge area bounded by the Urals in the west, the Pacific Ocean in the east, the Siberian continent in the north and the Tarim and North China continents in the south (Fig. 1a inset). This orogenic belt underwent a prolonged accretionary history, which probably started with the birth of the Paleo-Asian Ocean (PAO) in the latest Mesoproterozoic (Dobretsov et al., 1995; Khain et al., 2002, 2003) and was terminated with the formation of

\* Corresponding author at: Department of Earth Sciences, The University of Hong Kong, Pokfulam Road, Hong Kong.

E-mail address: [minsun@hku.hk](mailto:minsun@hku.hk) (M. Sun).

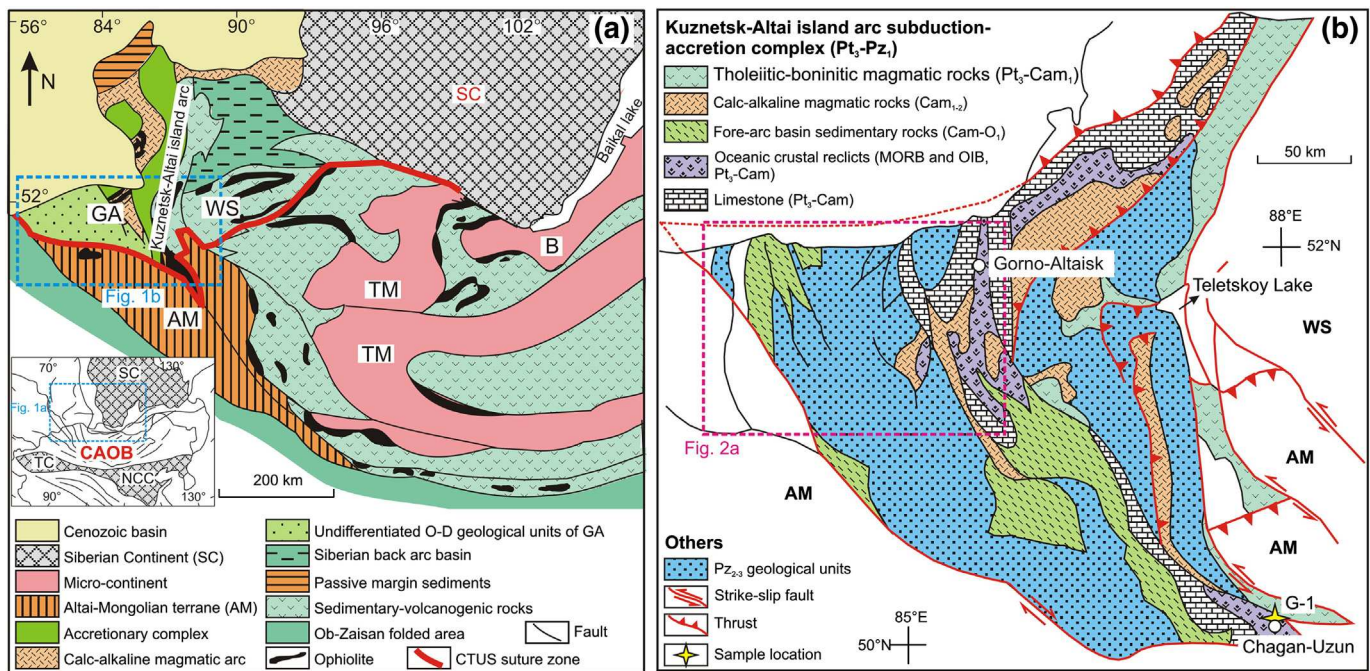


**Fig. 1.** (a) Simplified geological map showing the tectonic framework of northwestern Central Asian Orogenic Belt (CAOB, modified after Buslov and Safonova (2010)). (a) Inset shows the location of the CAOB. (b) The major structure units composing the Gorny Altai terrane (GA, modified after Ota et al., 2007). Abbreviations: TC, Tarim continent; NCC, North China continent; TM, Tuvo–Mongolian terrane; WS, West Sayan; B, Barguzin; CTUS, Charysh–Terekta–Ulagan–Sayan; Pt, Proterozoic; Pz, Paleozoic; Cam, Cambrian; O, Ordovician; D, Devonian.

the Southern Tianshan and Solonker suture zones in the late Paleozoic to early Mesozoic (Charvet et al., 2007; Wang et al., 2007; Xiao et al., 2003, 2009a, 2010). An archipelago model is now favored by most researchers, suggesting that various island arcs, ophiolites, accretionary prisms, oceanic plateaus and possibly some micro-continents were docked laterally due to the progressive multiple subduction–accretion processes (Badarch et al., 2002; Berzin and Kungurtsev, 1996; Berzin et al., 1994; Buslov et al., 2001, 2002, 2013; Dobretsov and Buslov, 2004; Dobretsov et al., 2013; Simonov et al., 1994; Wilhem et al., 2012; Windley et al., 2007; Xiao et al., 2004, 2009a,b, 2010; Zonenshain et al., 1990). Voluminous juvenile magmatic rocks were generated during the formation of the CAOB, making it the most important site of Phanerozoic crustal growth on the Earth (Buslov, 2011; Dobretsov and Buslov, 2007; Dobretsov et al., 2013; Jahn et al., 2000; Sun et al., 2008; Wu et al., 2000; Yuan et al., 2007). However, controversies exist on the nature of some important terranes, the mechanism of crustal growth and the proportion of the juvenile component (Buslov, 2011; Cai et al., 2011; Dobretsov et al., 2013; Jahn, 2004; Jahn et al., 2000, 2001a,b; Kovalenko et al., 2004; Kröner et al., 2014).

The Gorny Altai terrane (GA, Fig. 1a), situated in the northwest of the CAOB, is generally considered to be part of a subduction–accretion complex built upon the Kuznetsk–Altai intra-oceanic island arc southwest off the Siberian continent (present coordinate; Buslov, 2011; Buslov et al., 2013; Dobretsov and Buslov, 2007; Dobretsov et al., 2013; Glorie et al., 2011). This island arc was thought to be initiated in the late Neoproterozoic, generating boninitic rocks and ophiolitic mélange in the east of the GA (Buslov et al., 2001, 2002; Ota et al., 2002, 2007; Simonov et al., 1994). No reliable geochronological data have been obtained for the early magmatism of this island arc besides an imprecise clinopyroxene Ar–Ar age of  $647 \pm 80$  Ma for one clinopyroxenite from the ophiolitic mélange (Ponomarchuk et al., 1993). Hornblendes from retrograded eclogites in the Chagan Uzun, southeast of the GA, yielded Ar–Ar ages of ca. 630–560 Ma (Buslov et al., 2002), which possibly attest that the initial subduction occurred prior to the latest Neoproterozoic. It was suggested that this island arc matured in the middle–late Cambrian and collided with the Siberian continent in the late Cambrian to early Ordovician (Buslov et al. (2002); Glorie et al. (2011); Kruk et al.

(2011) and references therein). However, most of the arc assemblages were strongly deformed and occur as separate pieces due to strike-slip faulting in the late Paleozoic (Buslov et al., 2001, 2003, 2004, 2013). Only a few early Paleozoic plutons are exposed in the east of the GA and they were dated with zircon U–Pb ages of ca. 540–480 Ma (e.g., Glorie et al., 2011; Kruk et al., 2007, 2011). Although much more early Paleozoic granitoid plutons crop out in the northern part of the Kuznetsk–Altai island arc (e.g., the Kuznetsk–Alatau and Gornaya Shoria regions), their origin and petrogenesis have not been well constrained due to the scarcity of geochemical and geochronological data (Rudnev et al., 2008, 2013). Therefore, further investigations are required to understand the tectono-magmatic history of the Kuznetsk–Altai island arc.

Previous studies have shown that detrital zircons possibly provide a valid representation of the magmatic record of their source region (e.g., Wu et al., 2010; Cawood et al., 2012). In this study, (meta-)sedimentary rocks from the Cambrian to early Devonian sedimentary sequences from the GA (Figs. 1b and 2) were collected for detrital zircon U–Pb and Hf isotopic analyses. The aim is to reveal the geodynamic evolution of the Kuznetsk–Altai island arc and its role in the formation of the northwestern CAOB.

## 2. Geological setting

The GA is a triangle-shaped tectonic unit that is separated from the West Sayan terrane (WS) in the east and the Altai–Mongolian terrane (AM) in the south by the Charysh–Terekta–Ulagan–Sayan (CTUS) suture zone (Fig. 1; Buslov et al., 2002, 2003, 2004, 2013). The northern extension of the GA is covered by the Cenozoic sediments of the Biya–Barnaul depression.

The oldest rock units in the GA are the tholeiitic–boninitic volcanic rocks, as well as the associated accretionary complexes, high-pressure (HP) metamorphic rocks and ophiolitic mélange in the east of this terrane (Buslov et al., 2002, 2003, 2004, 2013; Ota et al., 2007). They were assigned to the late Neoproterozoic to early Cambrian based on stratigraphic and structural investigation (Buslov et al., 2001, 2002, 2013; Ota et al., 2007) and were thought to form during the initial stage of the Kuznetsk–Altai intra-oceanic island arc (Buslov et al.,

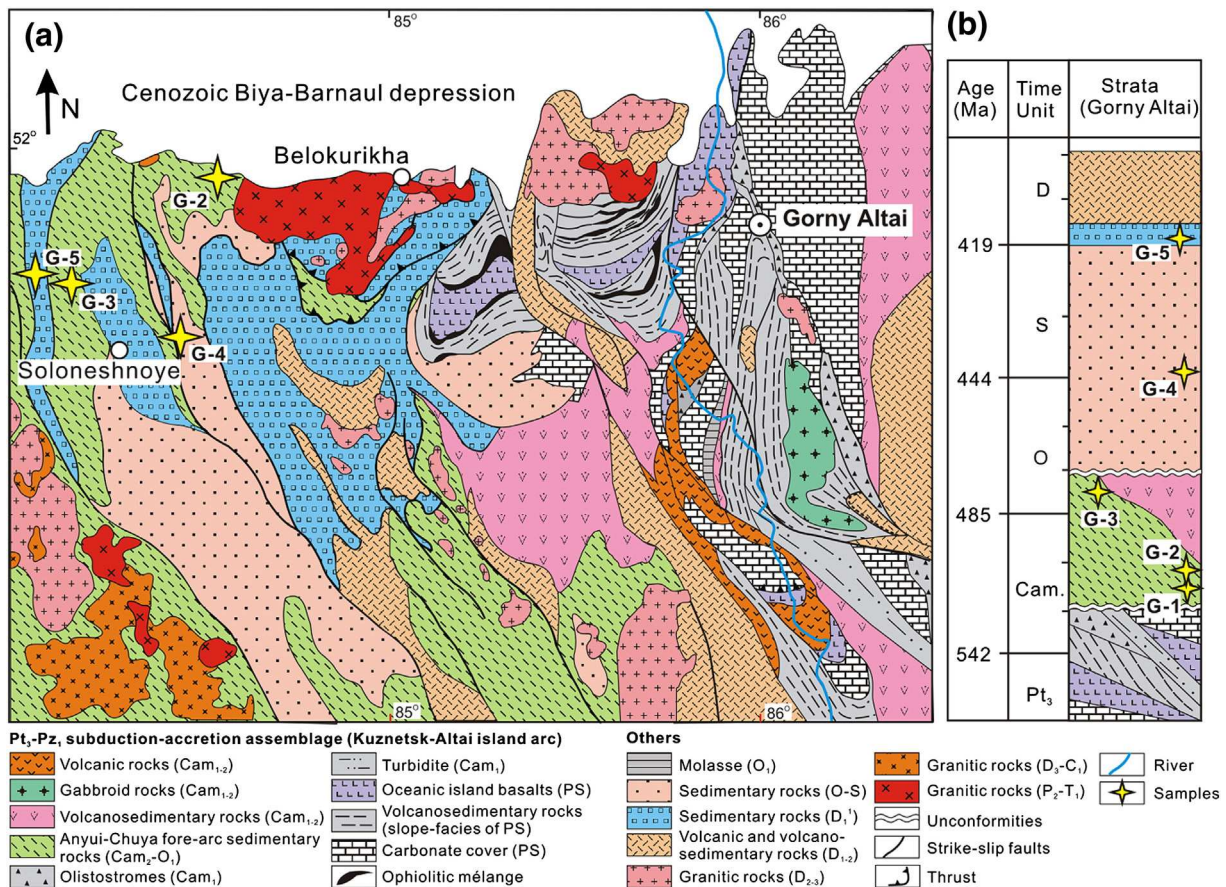


**Fig. 2.** (a) Geological units in the north of the GA (modified after Buslov et al. (2013)). (b) Simplified stratigraphic column in the north of the GA (based on geological maps of Buslov and Safonova (2010) and Buslov et al. (2013)). Abbreviations: Pt, Proterozoic; Pz, Paleozoic; Cam, Cambrian; O, Ordovician; S, Silurian; D, Devonian; P, Permian; C, Carboniferous; T, Triassic; PS, Paleo-seamount.

2001, 2002; Ota et al., 2002, 2007). The accretionary complexes consist mainly of oceanic crustal relicts with OIB- or MORB-like geochemical features and clastic rocks eroded from island arc magmatic rocks, ophiolitic mélange and HP metamorphic complexes (Buslov and Watanabe, 1996; Buslov et al., 2013; Dobretsov and Buslov, 2004; Ota et al., 2002, 2007; Safonova, 2008; Safonova et al., 2004, 2011). The limestone covers of paleo-seamounts (OIB-type oceanic crust) in the Kurai and Katun accretionary wedges yielded Pb–Pb ages of 598–577 Ma (Uchio et al., 2001, 2004), which are broadly consistent with the finding of early Cambrian algae and sponge spicules in the northern GA (Terleev, 1991). The eclogites in Chagan–Uzun (southeast of the GA) were formed by the subduction of oceanic crust and yielded hornblende Ar–Ar ages of ca. 630–560 Ma (Buslov et al., 2002). The Kuznetsk–Altai island arc was suggested to be mature with generation of calc-alkaline magmatism in the middle–late Cambrian (Glorie et al., 2011; Kruk et al., 2011; Simonov et al., 1994). A large turbidite basin was possibly formed in this period and the sedimentary sequences were assigned to the Gornyy Altai Group (Kruk et al., 2010). Its lower part consists of the Kudaty and Katun Formations that are predominantly composed of green–gray medium- to fine-grained sandstones and meta-siltstones (Kruk et al., 2010). The upper part consists of the Kadrinka, Sailyugem and Suetka Formations and is made up of poorly sorted coarse-grained immature sediments with greywacke compositions (Kruk et al., 2010). In the northwest of the GA, the upper limit of the Gornyy Altai Group is unconformably overlain by the Voskresenka Formation, which was assigned to the lower Ordovician (Petrunina et al., 1984). It was suggested that the Kuznetsk–Altai island arc collided with the Siberian continent in the late Cambrian to early Ordovician, resulting in the formation of molasse covering the Cambrian

sedimentary sequence (Fig. 2; Buslov et al., 2013), associated with intrusion of granitoids and folding (Buslov et al. (2002) and references therein).

The GA was suggested to represent a passive margin in the Ordovician to early Devonian when thick terrigenous-carbonate sediments were accumulated (Figs. 1b and 2; Buslov et al., 2013; Kruk et al., 2011). The Ordovician sedimentary sequences (4.5–6.0 km thick) are mainly composed of conglomerate, sandstone, siltstone and limestone. The Silurian sequences (1.5–2.0 km thick) conformably overlie the Ordovician ones and are dominated by carbonates with subordinate terrigenous sediments (Buslov et al., 2013; Yolkin et al., 1994).

In the Devonian, extensive granitoids, rhyolite–dacite lava and tuffs were generated and plutons intruded into the late Neoproterozoic to early Paleozoic sedimentary sequences (Fig. 2; Buslov, 2011; Buslov et al., 2013; Glorie et al., 2011; Kruk et al., 2011). This magmatic activity probably attests to the change of the geodynamic setting into an active continental margin (e.g., Glorie et al., 2011; Kruk et al., 2011). It was suggested that the AM collided with the marginal units of the Siberian continent (i.e., the GA) in the late Devonian to early Carboniferous, forming the CTUS suture zone (e.g., Buslov, 2011; Buslov et al., 2013).

### 3. Sample description

Five samples from the Cambrian to early Devonian sedimentary sequences (Figs. 1b and 2) in the GA were collected for zircon U–Pb and Hf-isotope analyses.

Samples G-1 (N 50°08'14.6", E 88°20'11.4"; Fig. 3a) and G-2 (N 51°59'18.5", E 84°33'52.4") were collected from the middle–late

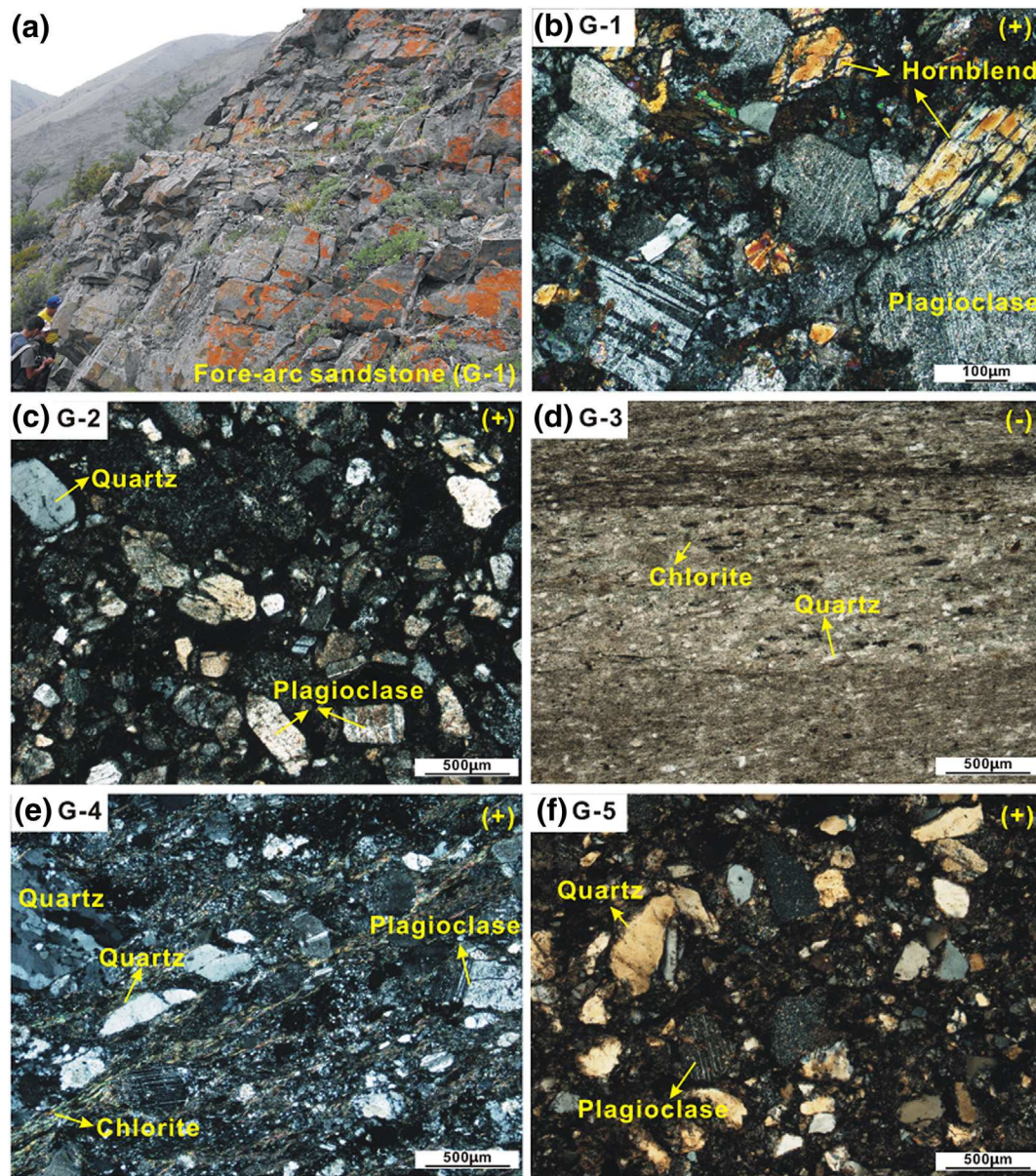


**Fig. 3.** The field occurrence (a) and petrography (b–f) of the representative (meta-)sedimentary rocks in the GA. (a) The early to middle Cambrian sandstone in the southeast of the GA (G-1); (b) G-1, coarse-grained sandstone, consisting of plagioclase, hornblende and quartz; (c) G-2, medium-grained plagioclase sandstone that is mainly composed of quartz and plagioclase, with minor lithic clastics; (d) G-3, greenschist-facies meta-siltstone, with a mineral assemblage of quartz + chlorite; (e) G-4, medium-grained sandstone that is dominated by quartz and plagioclase, with minor chlorite that was probably altered from pre-existed mafic minerals; (f) G-5, medium-grained sandstone that is mainly composed of quartz, plagioclase and lithic clastics. The symbols “(–)” and “(+)” in the up right angles of each diagram represent plane-polarized light and perpendicular polarized light, respectively.

Cambrian and late Cambrian to early Ordovician fore-arc sedimentary sequences of the Gornyy Altai Group in the southeast and northwest of the GA (Figs. 1b and 2), respectively. Sample G-1 is a coarse-grained sandstone, mainly composed of plagioclase (~60%), hornblende (~35%) and fine-grained matrix minerals (~5%) (Fig. 3b). All the minerals have subhedral to euhedral crystal shapes, indicating proximal sediment sources. Sample G-2 is a medium-grained sandstone, mainly composed of plagioclase (~70%), quartz (20%), lithic fragments (8%) and minor opaque minerals (~2%) (Fig. 3c). The minerals are also subhedral to euhedral.

Sample G-3 (N 51°48′38.5″, E 84°08′30.8″) was collected from the late Cambrian to early Ordovician fore-arc sedimentary sequences of the Gornyy Altai Group in the northwest of the GA (Fig. 2). It is a greenschist-facies meta-siltstone and is composed of quartz (~50%), chlorite (~45%) and minor opaque minerals (~5%). These minerals align along a preferred orientation and show clear foliation (Fig. 3d).

Sample G-4 (N 51°42′32.8″, E 54°25′27.8″) is a medium-grained sandstone from the Silurian sedimentary sequence in the northwest of the GA (Fig. 2). It consists of quartz (~70%), plagioclase (~20%), lithic fragments (~5%) and minor chlorite (~5%, altered from primary mafic minerals) (Fig. 3e).

Sample G-5 (N 51°50′32.3″, E 84°02′13.9″) is a medium-grained sandstone from the early Devonian sedimentary sequence in the northwest of the GA (Fig. 2) and has a similar mineral composition with the above-mentioned Silurian sample (Fig. 3f).

#### 4. Analytical methods

##### 4.1. Zircon separation and cathodoluminescence (CL) imaging

Rock samples were processed firstly by crushing, sieving, washing, and then by electromagnetic and standard heavy liquid separation.

About 100–200 zircon grains from each sample were handpicked from the heavy mineral concentrate under a binocular microscope. Being mounted in epoxy blocks, these zircon grains were polished down to about half of their thickness. CL imaging of the representative zircon grains was carried out in the Department of Earth Sciences, the University of Hong Kong in order to determine position for U–Pb and Hf-isotope analyses.

#### 4.2. In-situ zircon U–Pb and Hf-isotope analysis

In-situ zircon U–Pb dating was carried out by employing a Nu Instruments MC-ICPMS equipped with a Resonetics Resolution M-50-HR Excimer Laser Ablation System in the Department of Earth Sciences, the University of Hong Kong. Detailed operating conditions and instrument parameters were described by Xia et al. (2011). Analyses were performed with a beam of ca. 30  $\mu\text{m}$ , 6-Hz repetition rate, which yielded a signal intensity of 0.03 V at  $^{238}\text{U}$  for the standard zircon 91500. Typical ablation time was 40 s for each measurement, resulting in pits of 30–40  $\mu\text{m}$  in depth. Masses 232, 208–204 were simultaneously measured in static-collection mode. Standard zircons 91500 and GJ were used as external standards and were analyzed twice before and after every 10 analyses. Integration of background and analytic signals, time-drift correction, and quantitative calibration for U–Pb dating were performed by software ICPMSDataCal (Liu et al., 2010). U–Th–Pb isotopic ratios reported by Wiedenbeck et al. (1995) were used for the zircon standard 91500. Concordia diagrams and probability density plots were made using Isoplot/Ex\_ver3 (Ludwig, 2003). The U–Pb dating results are presented in Appendix Table S1.

Zircon Hf-isotope analyses were carried out by employing the same MC-ICPMS in the Department of Earth Sciences, the University of Hong Kong. Analyses were performed with a beam diameter of ca. 55  $\mu\text{m}$ , 6 Hz repetition rate, which yielded a signal intensity of 0.04 V at  $^{179}\text{Hf}$  for the standard zircon 91500. Typical ablation time was 40 s for each measurement, resulting in pits of 30–40  $\mu\text{m}$  in depth. Masses 172–179 were simultaneously measured in static-collection mode. Standard zircons 91500 and GJ were used as external standards and were analyzed twice before and after every 10 analyses. Data were normalized to  $^{179}\text{Hf}/^{177}\text{Hf} = 0.7325$ , using exponential correction for mass bias. Interference of  $^{176}\text{Lu}$  on  $^{176}\text{Hf}$  was corrected by measuring the intensity of the interference-free  $^{175}\text{Lu}$  isotope and using the recommended  $^{176}\text{Lu}/^{175}\text{Lu}$  ratio of 0.02655 (Machado, 2001). The  $^{176}\text{Lu}$  decay constant of  $1.865 \times 10^{-11} \text{ year}^{-1}$  (Scherer et al., 2001) was used to calculate initial  $^{176}\text{Hf}/^{177}\text{Hf}$  ratios. The chondritic values of  $^{176}\text{Hf}/^{177}\text{Hf}$  (0.282772) and  $^{176}\text{Lu}/^{177}\text{Hf}$  (0.0332) reported by Blichert-Toft and Albarède (1997) were adopted for the calculation of  $\epsilon_{\text{Hf}}(t)$  values. The two-stage Hf model ages ( $T_{\text{DM2}}$ ) were calculated using the Hf isotopic compositions of the depleted mantle ( $^{176}\text{Lu}/^{177}\text{Hf} = 0.0384$ ,  $^{176}\text{Hf}/^{177}\text{Hf} = 0.283250$ ) and average continental crust ( $^{176}\text{Lu}/^{177}\text{Hf} = 0.015$ ,  $f_{\text{Lu}/\text{Hf}} = -0.55$ ) reported by Griffin et al. (2000, 2002). The Hf isotope results are presented in Appendix Table S2.

## 5. Results

### 5.1. Zircon U–Pb and Hf isotopic compositions

#### 5.1.1. Sample G-1

Zircons from this sample are subhedral to euhedral, with typical oscillatory zoning (Fig. 4a). Their grain sizes vary from about 100 to 300  $\mu\text{m}$  in length, with length/width ratios mostly of ca. 1.0 to 1.5. The one hundred and six analyzed zircon grains yielded Th/U ratios between 0.15 and 1.07 (Appendix Table S1), suggesting a magmatic origin (Corfu et al., 2003; Hanchar and Miller, 1993). All the analyzed zircons give concordant or nearly concordant ages (Fig. 5a). Among them, ninety-nine grains have  $^{206}\text{Pb}/^{238}\text{U}$  ages clustering at 526–487 Ma, with a prominent peak at ca. 503 Ma (Fig. 6a). The other seven grains give  $^{206}\text{Pb}/^{238}\text{U}$  ages varying from 641 to 549 Ma. Eighty-one zircons out of

the one hundred and six were analyzed for Hf isotopic compositions, and they yield positive  $\epsilon_{\text{Hf}}(t)$  values (+3.8 to +16.1) and young  $T_{\text{DM2}}$  ages (1.32–0.45 Ga) (Fig. 7a; Appendix Table S2).

#### 5.1.2. Sample G-2

Most of the zircons from this sample are subhedral to euhedral with short prismatic shape. They have length/width ratios around 1.0 to 2.0 (Fig. 4b). All the thirty-nine analyzed zircons are characterized by concentric oscillatory zoning and Th/U ratios of 0.17–1.00, implying a magmatic origin (Corfu et al., 2003). Three zircon grains (G-2-1, G-2-40 and G-2-42) yield concordance less than 95% (Fig. 5b; Appendix Table S1). Among the other thirty-six zircons, zircon grain G-2-16 gives a  $^{206}\text{Pb}/^{238}\text{U}$  age of  $575 \pm 6$  Ma and the rest thirty-five grains yield  $^{206}\text{Pb}/^{238}\text{U}$  ages of 529–464 Ma (Fig. 6b). All these zircons have positive  $\epsilon_{\text{Hf}}(t)$  values varying from +3.4 to +15.5 and two-stage Hf model ages ( $T_{\text{DM2}}$ ) ranging from 1.27 to 0.50 Ga (Fig. 7b; Appendix Table S2).

#### 5.1.3. Sample G-3

Zircons from this sample are transparent and pale brown with euhedral to subhedral short prismatic shapes. The grain sizes vary from 150 to 300  $\mu\text{m}$  in length, with length/width ratios of ca. 1.0–2.5. CL images show that almost all the analyzed zircons exhibit oscillatory zoning (Fig. 4c). The one hundred and twenty-three analyzed zircon grains mostly yield concordance more than 95%. Zircon grains G-3-110, G-3-120 and G-3-122 yield concordant ages of  $613 \pm 6$  Ma,  $1947 \pm 7$  Ma and  $820 \pm 13$  Ma, respectively (Fig. 5c). Two zircon grains G-3-83 and G-3-112 give younger concordant  $^{206}\text{Pb}/^{238}\text{U}$  ages of ca. 339–328 Ma. They are characterized by uniform CL internal structure without zoning, possibly suggesting thermal disturbance in the late Paleozoic (Buslov et al., 2013). The other zircons give ages clustering at ca. 530–468 Ma (Fig. 6c). Among the one hundred and nine zircons that were analyzed with Hf isotopes, the three older zircons G-3-110, G-3-120 and G-3-112 yield negative  $\epsilon_{\text{Hf}}(t)$  values of  $-11.7$ ,  $-1.4$  and  $-3.4$ , with corresponding two-stage Hf model ages ( $T_{\text{DM2}}$ ) of  $2286 \pm 68$  Ma,  $2645 \pm 60$  Ma and  $1920 \pm 63$  Ma, respectively. Zircons of the major ca. 530–453 Ma population possess positive  $\epsilon_{\text{Hf}}(t)$  values of 1.7–13.9 and correspondingly  $T_{\text{DM2}}$  of 1.28–0.60 Ga, except for the zircon G-3-87 (ca. 503 Ma) with negative  $\epsilon_{\text{Hf}}(t)$  values of  $-5.9$  and  $T_{\text{DM2}}$  of  $1838 \pm 63$  Ma (Fig. 7c; Appendix Table S2).

#### 5.1.4. Sample G-4

Nearly all zircons from this sample are short and prismatic in shape and characterized by relatively wide oscillatory zoning in CL images (Fig. 4d). The Th/U ratios of these zircons are 0.12 to 0.80, indicating a magmatic origin (Corfu et al., 2003; Hanchar and Miller, 1993). Ninety-seven zircon grains were analyzed. Except for zircon grains G-4-40, G-4-88 and G-4-99, others all yield concordance more than 95% (Fig. 5d) and give  $^{206}\text{Pb}/^{238}\text{U}$  ages mainly concentrating at 555–456 Ma (Fig. 6d). Sixty representative zircon grains were analyzed for Hf isotopic compositions. They are characterized by positive  $\epsilon_{\text{Hf}}(t)$  values from +6.6 to +17.5 (Fig. 7d; Appendix Table S2). Except for zircon G-6-51 with the two-stage Hf model age ( $T_{\text{DM2}}$ ) of 0.34 Ga, others yield model ages of 1.03–0.51 Ga.

#### 5.1.5. Sample G-5

Zircons from this sample are short prismatic or sub-rounded in shape, with length/width ratios varying from ca. 1.0 to 1.5 (Fig. 4e). They are mostly characterized by well oscillatory zoning and Th/U ratios from 0.09 to 2.29, implying a magmatic origin (Corfu et al., 2003; Hanchar and Miller, 1993). Among the eighty analyzed zircon grains, zircons G-5-12, G-5-24, G-5-39 and G-5-60 give concordant or nearly concordant  $^{207}\text{Pb}/^{206}\text{Pb}$  ages of 2431–1879 Ma (Fig. 5e). Zircon grains G-5-7, G-5-17, G-5-20, G-5-50, G-5-57 and G-5-64 yield concordant ages varying from 904 Ma to 772 Ma (Fig. 5e). Other zircons give concordant  $^{206}\text{Pb}/^{238}\text{U}$  ages mainly clustering between 525 Ma and

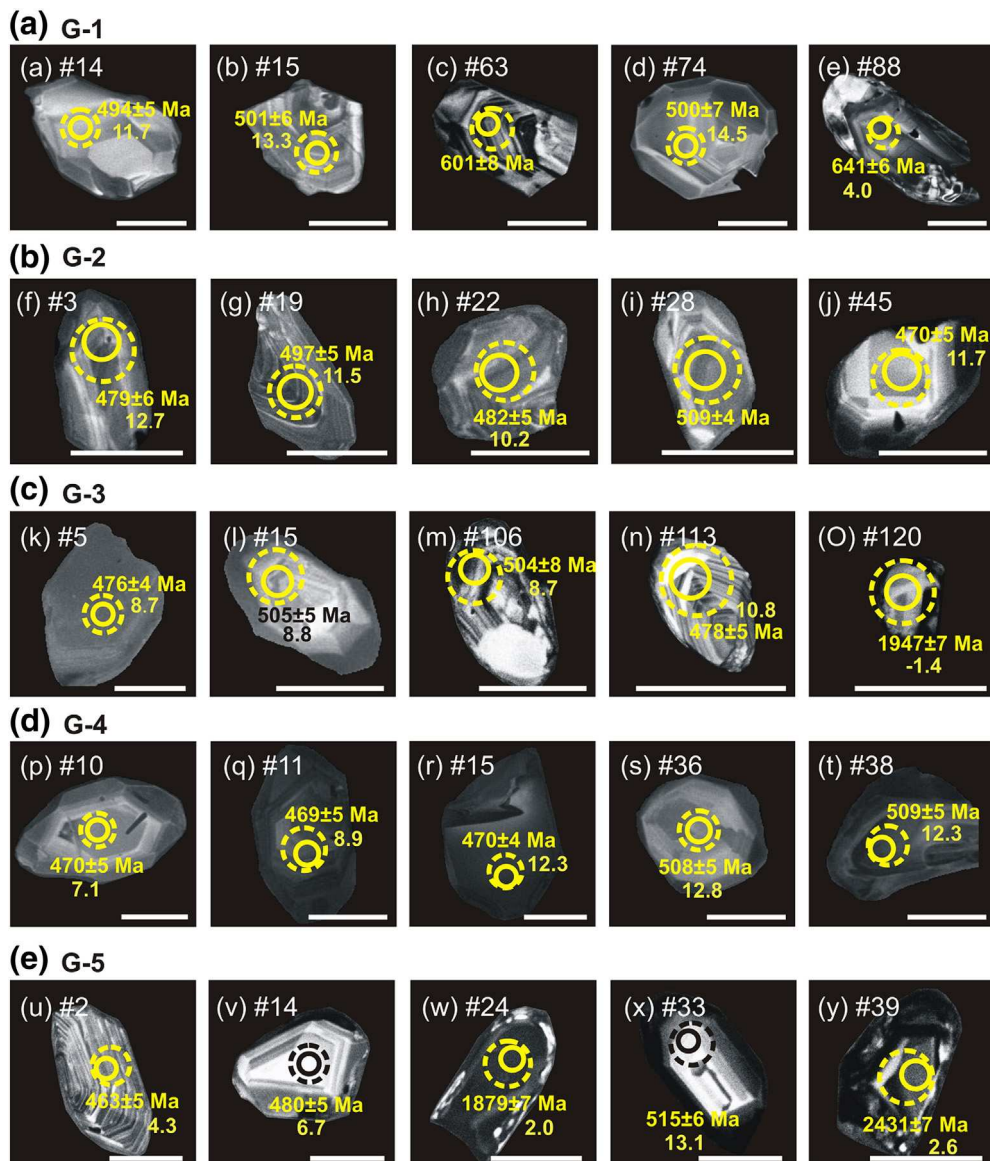


**Fig. 4.** CL images of representative zircon grains from the sedimentary rocks. The scale bars are 100  $\mu\text{m}$  in length. The circles marked with dashed lines and solid lines are the spots for zircon U–Pb dating and HF-isotope analyses, respectively. The corresponding results are presented in Appendix Table S1 and S2.

463 Ma except for the grains G-5-23, G-5-49 and G-5-65 with ages of 632–592 Ma (Fig. 6e). Similar to other four samples, the early Paleozoic zircons (525–463 Ma) from sample G-5 are dominated by positive  $\varepsilon_{\text{Hf}}(t)$  values from +1.0 to +14.9 and correspondingly give  $T_{\text{DM2}}$  model ages of 1.40–0.52 Ga; only zircons G-5-31, G-5-38 and G-5-47 yield negative  $\varepsilon_{\text{Hf}}(t)$  values (–3.3 to –9.3) and  $T_{\text{DM2}}$  model ages of 2.06–1.66 Ga (Fig. 7e; Appendix Table S2). In contrast, those Precambrian zircons show extremely varied initial Hf isotopic compositions, with  $\varepsilon_{\text{Hf}}(t)$  values and  $T_{\text{DM2}}$  model ages varying from –26.1 to +11.7 and 3.74 to 0.82 Ga, respectively.

## 6. Discussion

### 6.1. The timing of deposition

The ages of the youngest detrital zircons have been successfully used to constrain the maximum depositional age of sedimentary rocks (e.g. Dickinson and Gehrels, 2009; Jones et al., 2009; Long et al., 2007). A recent study shows that the youngest peak age of probability density plot (YPP) or a mean age of the youngest-grain cluster ( $n \geq 2$ )

overlapping in age at 1 sigma ( $YC1\sigma(2+)$ ) can provide a reliable estimation of the youngest-age measures (Dickinson and Gehrels, 2009). In this study, we adopt the  $YC1\sigma(2+)$  to constrain the timing of deposition, as used by some other researchers (e.g. Jones et al., 2009).

The eighty youngest concordant or nearly concordant detrital zircons (ca. 512–487 Ma) from sample G-1 yield an average age of  $502 \pm 1$  Ma (MSWD = 1.00 ( $2\sigma$ )), constraining a maximum deposition age in the middle Cambrian. Similarly, the twelve and thirty-eight youngest concordant or nearly concordant detrital zircons from samples G-2 and G-3 (ca. 477–464 Ma and 481–468 Ma, respectively) show weighted mean ages of  $472 \pm 3$  Ma (MSWD = 0.95 ( $2\sigma$ )) and  $476 \pm 1$  Ma (MSWD = 1.00 ( $2\sigma$ )), respectively, suggesting that they were deposited in no earlier than early Ordovician. Our results suggest that the Gorny Altai group (represented by samples G-1, G-2 and G-3) received sediments at least till ca. 472 Ma. Sample G-4 was collected from a Silurian sequence that was constrained by graptolite fossils in the shale from the lower part of the same section (Yolkin et al., 1994). The forty-seven youngest concordant or nearly concordant detrital zircons (ca. 476–456 Ma) have an average age of  $467 \pm 1$  Ma (MSWD = 1.03 ( $2\sigma$ )). This implies that the host sedimentary sequence probably deposited

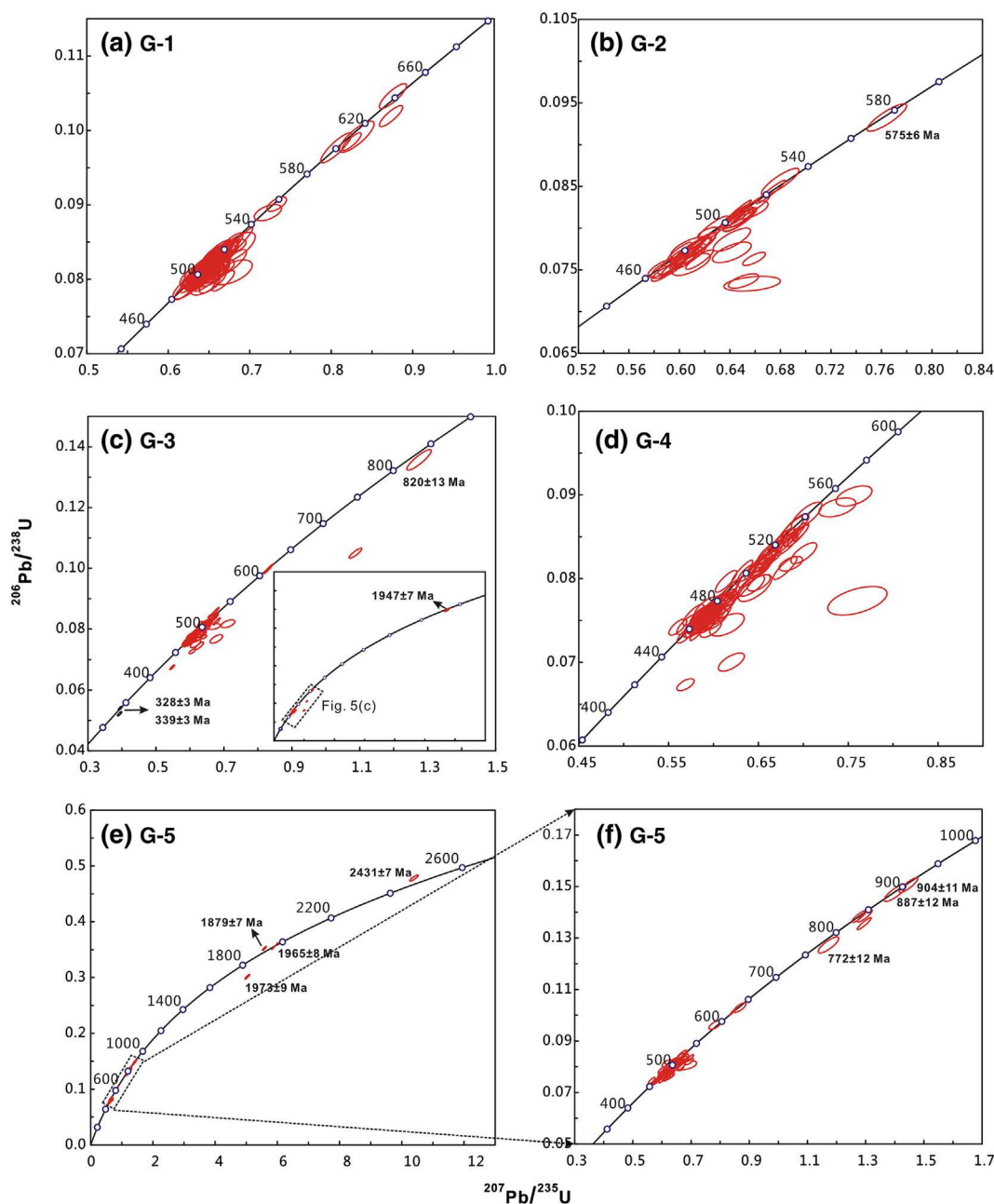


Fig. 5. U–Pb concordia diagrams for detrital zircons from the (meta-)sedimentary rocks in the GA.

in no earlier than the middle Ordovician, which is compatible with the previously assigned age of Silurian. The nine youngest concordant or nearly concordant detrital zircons from the early Devonian sample G-5 (ca. 475–463 Ma) overlapping in age at 1 sigma have an average age of  $469 \pm 3$  Ma (MSWD = 1.02 ( $2\sigma$ )). This age constrains the maximum deposition time in the middle Ordovician and thus is also compatible with the assigned age of early Devonian (Fig. 2; Buslov et al., 2013 and reference therein).

## 6.2. Provenance

Detrital zircons are common in sedimentary rocks and have been widely applied in tracing the provenance of sedimentary systems (e.g. Barth et al., 2013; Cawood et al., 2012; Wu et al., 2010).

The three samples of the Gorny Altai Group (i.e., G-1, G-2 and G-3) show detrital zircons mainly of 530–464 Ma old, with minor 641–549 Ma old (Fig. 6a–c). These zircons retain euhedral to subhedral

morphology, oscillatory concentric zoning (Fig. 4) and high Th/U ratios (Appendix Table S1), implying a magmatic origin with short-distance transport (Corfu et al., 2003; Hanchar and Miller, 1993). This conclusion can be further supported by the preservation of euhedral to subhedral mafic minerals (i.e. hornblende) in sample G-1 (Fig. 3b) and the observation of poorly sorted plagioclase and quartz with angular shapes in sample G-2 (Fig. 3c). The Kuznetsk–Altai intra-oceanic island arc (Fig. 1) is located in the east of the sampling sites. This arc is dominated by the assumed late Neoproterozoic to early Cambrian tholeiitic–boninitic volcanic rocks and Cambrian calc-alkaline magmatic rocks (Fig. 1b; Buslov et al. (2002); Ota et al. (2007) and references therein). A few granitoid–gabbro–tonalite plutons in the east of the GA (the southern part of the Kuznetsk–Altai island arc; Kruk et al., 2007, 2011; Glorie et al., 2011) as well as the Kuznetsk–Alatau and Gornaya regions (the northern part of the Kuznetsk–Altai island arc; Rudnev et al., 2008, 2013) have been recently dated with zircon U–Pb ages of ca. 540–480 Ma (De Grave et al., 2009; Glorie et al., 2011; Kruk et al., 2007;

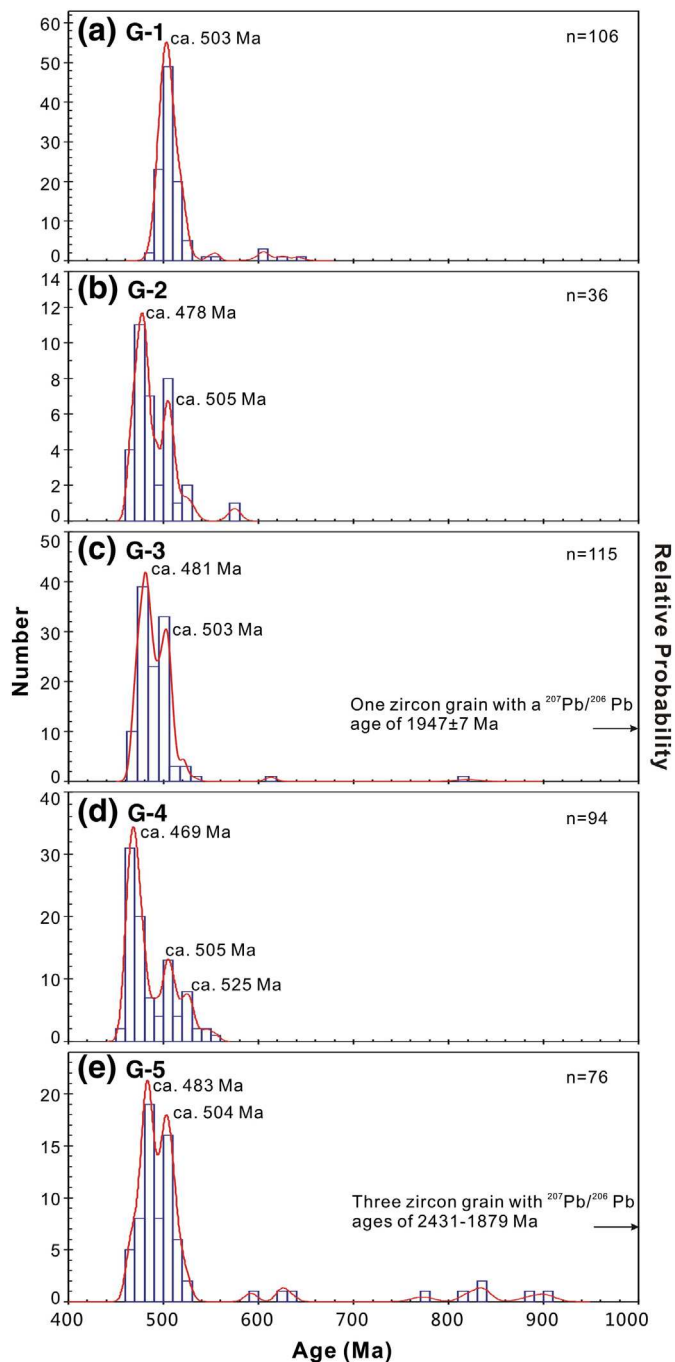


Fig. 6. Histogram of zircon ages for each of the studied (meta-)sedimentary rocks in the GA.

Rudnev et al., 2013), which are broadly coeval with the dominant detrital zircon populations in our samples. The uniform detrital zircon patterns without early Precambrian grains suggest that the Kuznetsk–Altai island arc magmatic rocks probably served as dominant sediment sources. Sample G-1 has youngest zircons slightly older than those of the other two samples, consistent with its stratigraphic position in the lower part of the Gornyy Altai Group (Fig. 2).

The Silurian and early Devonian sedimentary sequences in the Anui-Chuya basin, represented by samples G-4 and G-5, respectively, were considered as passive marginal deposits of the Siberian continent (Buslov and Safonova, 2010; Buslov et al., 2013). Studies have revealed that detrital zircons from passive margin sedimentary sequences of an ancient continent usually contain a significant proportion of ancient

grains as a result of sediments sourced from this continent (Cawood et al., 2012). However, detrital zircons from the Silurian sample G-4 show a single population with ages mainly of 555–456 Ma (Fig. 6d) and thus were possibly derived from sources similar to those of the Gornyy Altai Group. This may imply that the GA was not directly connected with an old continent in the Silurian. In contrast, 2431–772 Ma zircons make up a significant proportion (ca. 12%) in the early Devonian sample G-5 in addition to the major zircon population of 525–463 Ma (ca. 84%) and a minor one of 632–592 Ma (ca. 4%) (Fig. 6e). These 2431–772 Ma zircons exhibit subhedral to rounded shapes with blurry oscillatory concentric zoning (Fig. 4e), which possibly imply far-distance transport. We consider that some detritus from ancient continents began to be involved in the formation of the early Devonian sedimentary sequences besides the 632–463 Ma magmatic rocks.

### 6.3. Implication on the Kuznetsk–Altai arc magmatism

As discussed above, the five investigated samples have detrital zircons predominantly from the nearby Kuznetsk–Altai island arc except the early Devonian one with a significant input of 2431–772 Ma detrital zircons from additional ancient continents. We propose that two different magmatic stages were possibly responsible for the formation of this island arc based on the contrasting zircon abundances (Fig. 8a).

#### 6.3.1. Primitive stage at ca. 640–540 Ma

In the latest Mesoproterozoic to Neoproterozoic, the southern and western margins of the Siberian continent (present coordinate) were surrounded by the PAO after the breakup of the Rodinia supercontinent (Dobretsov et al., 1995; Khain et al., 2002, 2003). Voluminous magmatic rocks were generated in association with the long-lasting subduction–accretion processes due to the closure of the PAO (e.g. Cai et al., 2010; Glorie et al., 2011; Kröner et al., 2014; Sun et al., 2008; Yuan et al., 2007). It was proposed that the primitive Kuznetsk–Altai island arc off the Siberian continent was initiated in the late Neoproterozoic to early Cambrian due to the transition from a transform fault zone to an incipient subduction zone, which is manifested by the tholeiitic–boninitic volcanic rocks in the GA (Buslov, 2011; Buslov et al., 2002, 2013; Ota et al., 2007). The eclogites that are associated with the ophiolitic mélange in the southeast of the GA yielded hornblende Ar–Ar ages of ca. 630–560 Ma (Buslov et al., 2002), indicating that the subduction possibly occurred prior to the latest Neoproterozoic. However, the timing of magmatism during this period has not been well understood due to the lack of precise geochronological data (Fig. 8b). The five samples of this study contain ca. 640–540 Ma detrital zircons, although in minor amount (ca. 5%; Fig. 8a), may testify that the precursor magmas of these zircons were generated in the primitive subduction stage of the Kuznetsk–Altai island arc. We explain that the scarcity of ca. 640–540 Ma detrital zircons is possibly because basalts and basaltic andesites were the major products during this period (e.g., Buslov et al., 2004; Ota et al., 2007) and zircons are difficult to crystallize in these kinds of magmas (Cawood et al., 2012 and references therein).

#### 6.3.2. Evolved stage at ca. 530–470 Ma

The seventy-eight youngest concordant or nearly concordant detrital zircons (except for zircons G-3-83 and G-3-112 with ages of 339–328 Ma) from the five samples show an average age of  $469 \pm 1$  Ma (MSWD = 0.95 ( $2\sigma$ )). This implies that the subduction-related magmatism possibly continued at least till ca. 470 Ma, rather than ca. 490–480 Ma that was inferred from the limited magmatic exposures (Fig. 8b; Buslov et al., 2002; De Grave et al., 2009; Glorie et al., 2011; Kruk et al., 2007, 2011; Rudnev et al., 2008, 2013). Compared with the low abundance of ca. 640–540 Ma detrital zircons, all the five samples show high fertility of ca. 530–470 Ma old populations (ca. 95%). This may imply that an increased volume of magmas with relatively high SiO<sub>2</sub> contents (e.g., granitoid and their volcanic equivalents) was generated in their source areas. Experimental studies show that granitoid



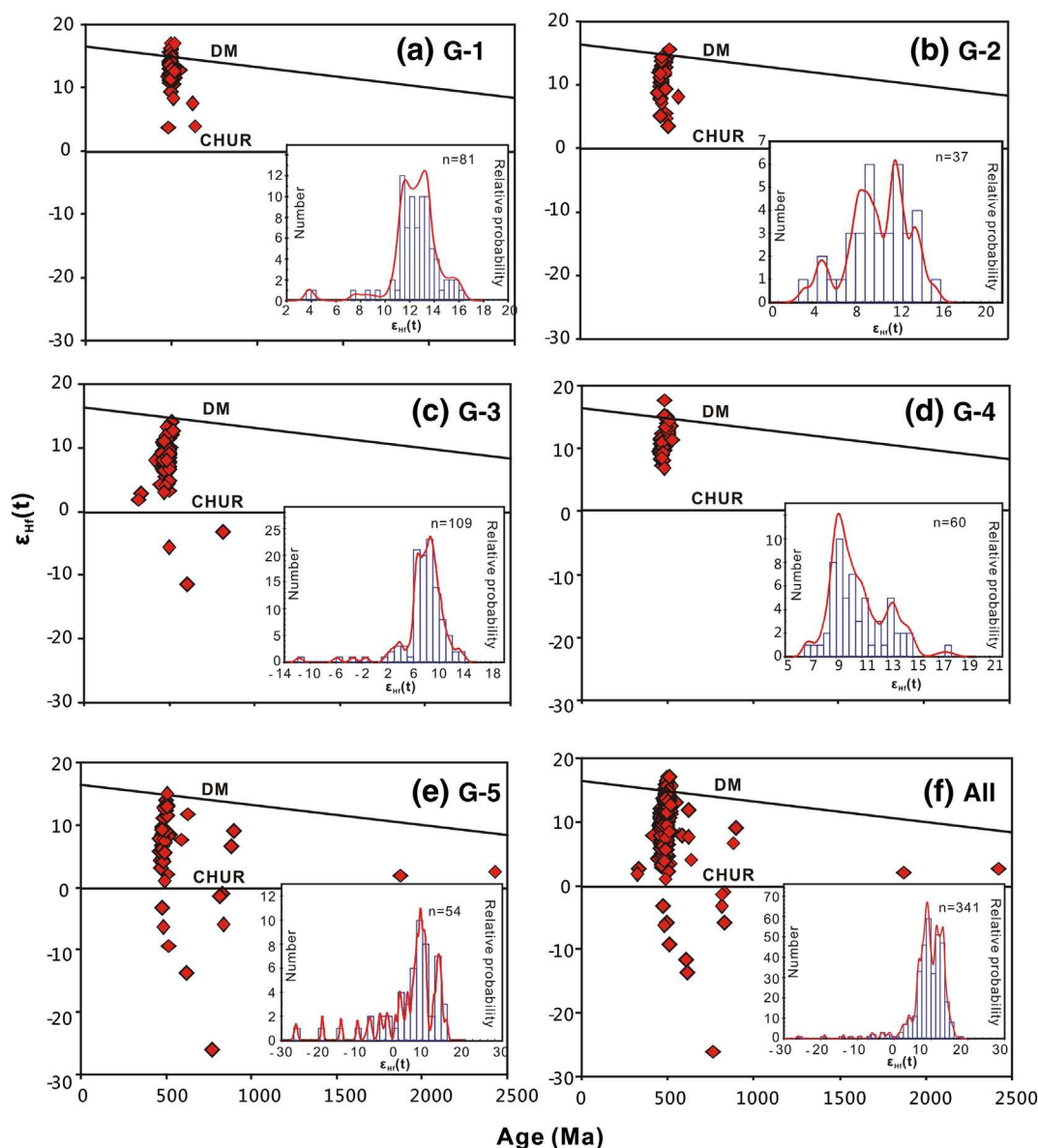


**Fig. 7.** Plots of age (Ma) versus  $\epsilon_{\text{Hf}}(t)$  for zircons from the (meta-)sedimentary rocks in the GA. The  $^{207}\text{Pb}/^{206}\text{Pb}$  ages are adopted for the crystallization age they are older than 1000 Ma, otherwise the  $^{206}\text{Pb}/^{238}\text{U}$  ages are adopted.

magmas and more felsic ones can be rarely produced solely by fractional crystallization of mantle-derived mafic melts, but are mostly generated by partial melting of crustal materials at middle and/or lower crustal depth (e.g., Cai et al. (2014) and references therein). The ca. 530–470 Ma detrital zircons are almost exclusively characterized by positive  $\epsilon_{\text{Hf}}(t)$  values varying from +1.0 to +18.9, with  $T_{\text{DM2}}$  ages mainly of 1.40–0.45 Ga (Figs. 7 and 9; Appendix Table S2). Therefore, our results may indicate that substantial partial melting of the pre-existing juvenile mafic crustal materials occurred in ca. 530–470 Ma. Recent studies show that the Cambrian to early Ordovician granitoids from the Kuznetsk–Altai island arc are mainly metaluminous to weakly peraluminous ( $A/\text{CNK} < 1.1$ , molar ratio,  $\text{Al}_2\text{O}_3/(\text{CaO} + \text{Na}_2\text{O} + \text{K}_2\text{O})$ ) in composition, with subordinate strongly peraluminous ( $A/\text{CNK} > 1.1$ ) ones (Fig. 10a; Kruk et al., 2011; Rudnev et al., 2008). Comparison with partial melting experiments shows that these two kinds of granitoids were predominantly originated from meta-basaltic igneous rocks and meta-sediments, respectively (Fig. 10b; Altherr et al. (2000) and references therein). The increased production of granitoids, which has been regarded as a distinctive feature of mature island arcs from

juvenile/primitive one (Baker, 1968), suggests that the Kuznetsk–Altai island arc probably evolved toward a mature one at ca. 530–470 Ma.

To conclude, the detrital zircons in this study provide a complete record of the tectono-magmatic evolution of the Kuznetsk–Altai island arc from ca. 640 to 470 Ma, indicating that considerable continental growth took place at least till in ca. 470 Ma. With combination of previously published data, we tentatively propose a scenario for the evolution of the Kuznetsk–Altai island arc as follows (stages A–C in Fig. 11). At ca. 640 Ma (stage A), the nascent Kuznetsk–Altai island arc was initiated, when the arc crust was possibly thin and dominated by basaltic magma flux from the depleted mantle (e.g., tholeiitic–boninitic volcanic rocks; Buslov et al., 2002; Ota et al., 2007). This island arc progressively became thickened due to the increased input of mantle-derived mafic magmas and growth of accretionary prism by ongoing subduction. When it came to ca. 530–470 Ma (stage B), partial melting of the deeply buried accretionary assemblages and oceanic crust generated relatively large amount of granitoids (e.g. Glorie et al., 2011; Kruk et al., 2011; Rudnev et al., 2008, 2013). Middle–late Ordovician zircons are missing in the Silurian sample (G-4, Fig. 6d). Similarly, middle Ordovician to

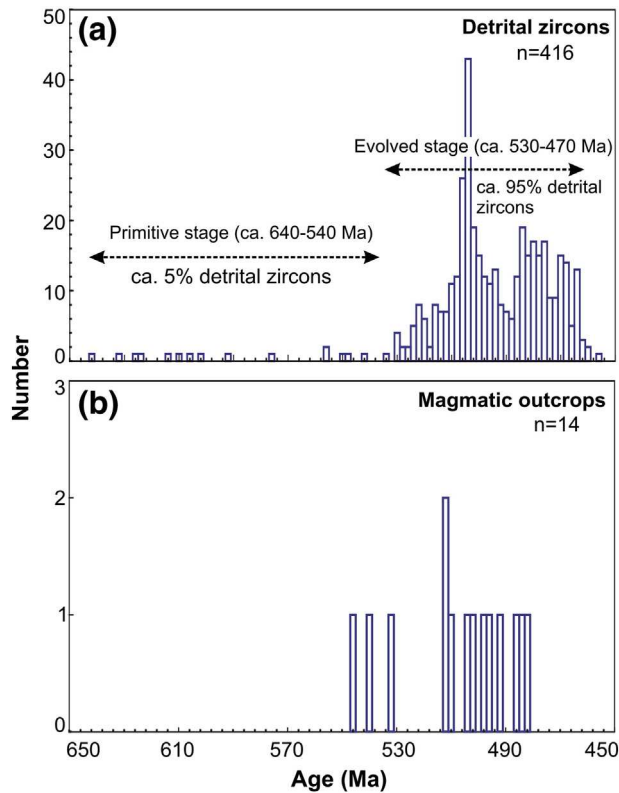


**Fig. 8.** Comparison between the detrital zircons (a) and magmatic outcrops (b) records on the magmatic history of the Kuznetsk–Altai island arc. The 2431–772 Ma detrital zircons are excluded for the reason that they were possibly derived from old continents (e.g., the Altai–Mongolian terrane). The U–Pb age data for the magmatic outcrops are from Kruk et al. (2007, 2011), Rudnev et al. (2008, 2013) and Glorie et al. (2011).

early Devonian zircons are not found in the early Devonian sample (G-5, Fig. 6e). This possibly implies that the GA changed into a passive regime (but probably not directly connected with any old continent) in the middle Ordovician (stage C).

#### 6.4. Sources of the 2431–772 Ma detrital zircons and their tectonic implication

The three samples from the Gorny Altai Group and one from the Silurian sedimentary sequence show predominant zircon populations

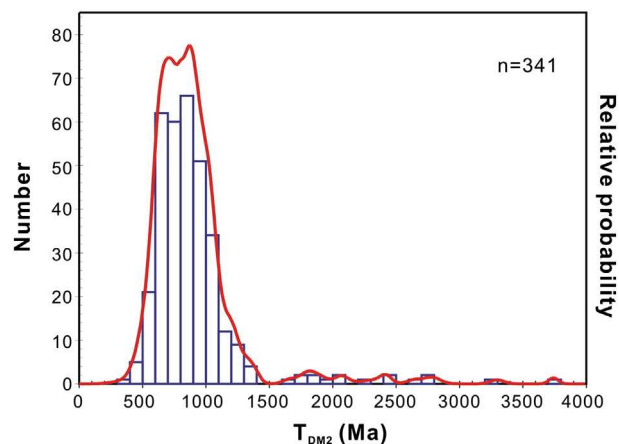


**Fig. 9.** Histogram of two-stage Hf-isotope model ages ( $T_{DM2}$ ) for all detrital zircons from the (meta-)sedimentary rocks in the GA.

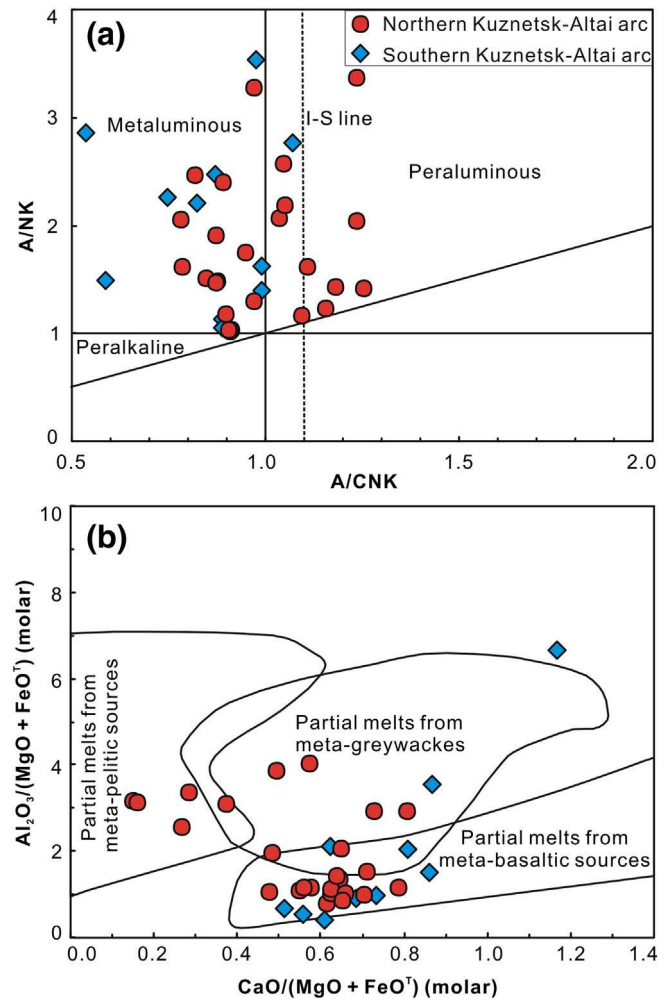


**Fig. 10.** Compilation of geochemical data about the Cambrian–Ordovician granitoids from the northern (i.e., the Kuznetsk Alatau area; Rudnev et al., 2008) and southern parts (i.e., the east of the Gorny Altai terrane; Kruk et al., 2011) of the Kuznetsk–Altai island arc. The I–S line in (a) is after Chappell and White (2001). The fields representing different kinds of partial melts in (b) are outlined after Altherr et al. (2000) and references therein.

with Cambrian to early Ordovician ages, without Archean to middle Neoproterozoic zircons (except for one of 1947 Ma and one of 820 Ma old, respectively). However, significant amount of 2431–772 Ma zircons appear in the early Devonian sample (G-5; Figs. 6e and 12a), and yield variable but mostly negative Hf isotopic compositions with  $T_{DM2}$  model ages up to 3.74 Ga. This indicates that a tectonic unit with old crustal material approached the GA near the early Devonian.

To the northeast of the GA is the Siberian continent, which is one of the oldest continental blocks on the Earth (Fig. 1a). The Paleozoic sediments and modern river sands from this continent are highlighted by ca. 35% 3.2–2.4 Ga and ca. 50% 2.1–1.8 Ga zircon populations (Fig. 12b; Gladkochub et al., 2013; Safonova et al., 2010; Wang et al., 2011), which are quite distinct from our data from the early Devonian sample (Fig. 12a). These two major zircon populations are explained to record the formation of continental nuclei in the Archean to early Paleoproterozoic and the amalgamation of these ancient nuclei in the middle–late Paleoproterozoic (e.g., Gladkochub et al., 2013; Rosen et al., 1994; Safonova et al., 2010; Wang et al., 2011). Early–middle Neoproterozoic magmatic rocks are only distributed in its southeastern and southern margins as a result of the early subduction–accretion processes during the formation of the CAOB (e.g., Vernikovskiy et al., 2003; Zonenshain et al., 1990). This is witnessed in the sedimentary record, where the early–middle Neoproterozoic detrital zircons only take up

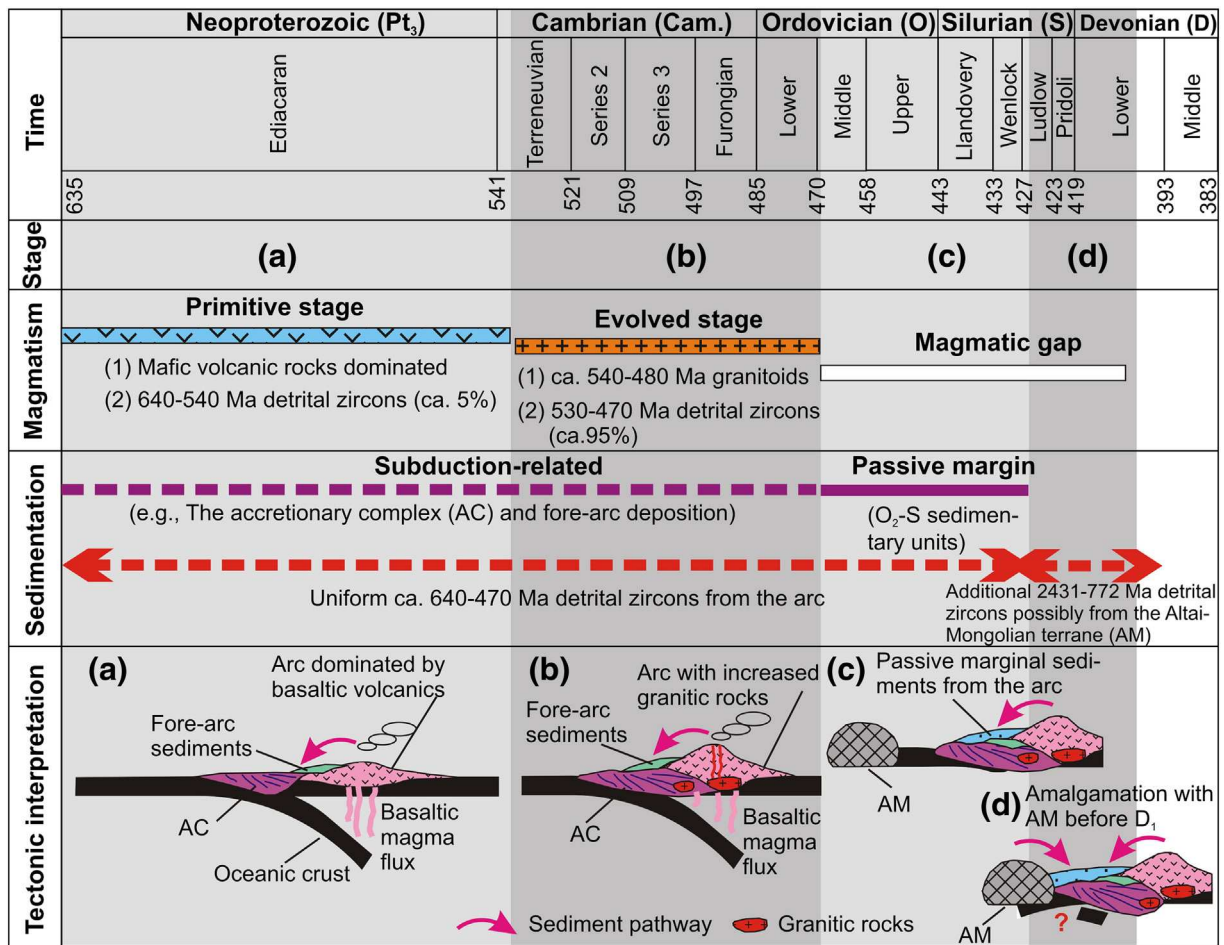


**Fig. 11.** A simplified sketch illustrating the magmatic evolution of the Kuznetsk–Altai island arc and the associated provenance change during sedimentation from the late Neoproterozoic to early Devonian. The time scale is referred from the Cohen et al. (2013). Data about the magmatic outcrops are cited in the text.

ca. 15% in the compiled  $\geq 640$  Ma grains (Fig. 12b). However, the 2431–772 Ma detrital zircons from our early Devonian sample G-5 are highlighted by more than 60% Neoproterozoic detrital grains, which are followed by a subordinate amount of the middle–late Paleoproterozoic ones (Fig. 12a). The pattern is quite different from that of the Siberian continent (Fig. 12d). Therefore, the Siberian continent seems unlikely to be a major source for the ancient sediments in the early Devonian sedimentary sequences.

We note that the Precambrian detrital zircons from the early Paleozoic meta-sedimentary rocks in the AM to the south of the GA mostly have Neoproterozoic ages and minor grains of them formed in the Archean to Paleoproterozoic (Fig. 12c; Chen et al., in press; Jiang et al., 2010, 2011, 2012; Long et al., 2007, 2010; Sun et al., 2008; Wang et al., 2014). Since no Precambrian basement is exposed on the AM, researchers suggested that these old detrital zircons were possibly derived from the Tuva–Mongolian terrane (e.g. Jiang et al., 2011; Long et al., 2010), where Precambrian rocks (e.g., ortho-gneisses) have been well documented (Badarch et al., 2002; Demoux et al., 2009; Jiang et al., 2011 and references therein). The  $\geq 640$  Ma detrital zircons from the AM include ca. 60% Neoproterozoic grains, ca. 30% middle–late Paleoproterozoic and ca. 10% Archean ones. This pattern is thus quite similar to that of the 2431–772 Ma grains from our early Devonian sample G-5 (Fig. 12d). We propose that the detritus from the AM are plausibly an additional source to the early Devonian sedimentary sequence. Previous studies suggested that the GA and AM were possibly amalgamated in the late Devonian to early Carboniferous, i.e., after the deposition of our early Devonian sample (Buslov, 2011; Buslov et al.,

2004, 2013). The upper limit of amalgamation time was constrained by the amphibole K–Ar age of the gabbro–diabase dykes (ca. 373 Ma) that penetrated the metamorphosed rocks in the suture (Buslov (2011) and references therein). However, the K–Ar age may record the timing of cooling related to the uplift along the shear zone. Our data may imply that the GA and AM amalgamated already in the early Devonian (stage D in Fig. 11).

## 7. Conclusions

- (1) Detrital zircons from the Gorny Altai Group and the Silurian sedimentary sequence all show the most prominent zircon population with Cambrian to early Ordovician ages, with a subordinate one with late Neoproterozoic ages. Detritus from the Kuznetsk–Altai island arc system probably served a unitary source in the formation of these sedimentary rocks.
- (2) The Kuznetsk–Altai island arc possibly underwent a prolonged tectono-magmatic history from ca. 640 Ma to ca. 470 Ma. Nearly all the ca. 530–470 Ma detrital zircons yield positive  $\varepsilon_{\text{Hf}}(t)$  values with  $T_{\text{DM2}}$  ages of ca. 1.40–0.45 Ga, implying that the precursor magmas were dominated by heterogeneous juvenile crustal materials. The low abundance of ca. 640–540 Ma detrital zircons implies that the Kuznetsk–Altai island arc was possibly a primitive one dominated by mafic volcanic rocks in this period, while the abrupt increase of the ca. 530–460 Ma ones possibly indicates that this arc evolved toward a mature one with substantial intermediate–felsic magmas (e.g., granitoids) in the

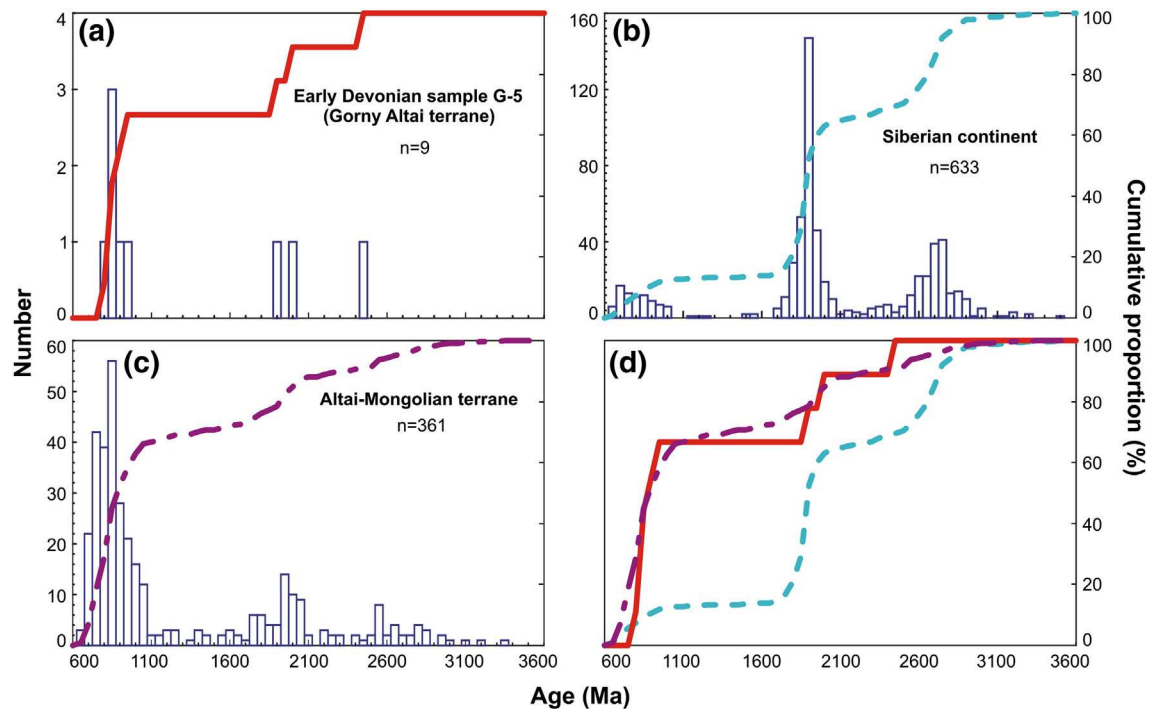


**Fig. 12.** Comparison between the 2431–772 Ma detrital zircons from the early Devonian sample G-5 and the Precambrian detrital zircon records ( $\geq 640$  Ma) from the Altai-Mongolian terrane and Siberian continent. The U–Pb age data for detrital zircons from the Altai-Mongolian terrane are from Long et al. (2007, 2010), Sun et al. (2008), Jiang et al. (2010, 2011, 2012), Yang et al. (2011), Chen et al. (in press) and Wang et al. (2014), while those from the Siberian continent are from Safonova et al. (2010), Wang et al. (2011) and Gladkochub et al. (2013).

Cambrian to early Ordovician.

- (3) The AM is a plausible source for the 2431–772 Ma detrital zircons in the early Devonian sample. This implies that the GA possibly amalgamated with the AM prior to the early Devonian rather than in the late Devonian to early Carboniferous as previously suggested.

Supplementary data to this article can be found online at <http://dx.doi.org/10.1016/j.lithos.2015.03.020>.

#### Acknowledgments

This study was financially supported by the Major Basic Research Project of the Ministry of Science and Technology of China (grant: 2014CB440801), the Hong Kong Research Grant Council (HKU705311P and HKU704712P), the National Science Foundation of China (41273048, 41190075), a HKU CRCG grant (201311159190) and the Siberian Branch of the Russian Academy of Sciences (basic research project no. VIII.66.1 of the IGM SB RUS and projects of the Presidium RAS no. 28.2). This work is a contribution of the Joint Laboratory of Chemical Geodynamics between HKU and CAS (Guangzhou Institute of Geochemistry), Germany/Hong Kong Joint Research Scheme and IGCP #592 Project “Continental construction in Central Asia”. Drs. Hongyan Geng and Jean Wong are thanked for their laboratory assistance. Arnaud Broussolle is also thanked for his help in polishing the English. The late Professor Rob Kerrich spent incredible time to mentor his students and young researchers. We were all benefited through our scientific career by his guidance, encouragement, and friendship. This paper is specially dedicated to Rob. We thank the two anonymous reviewers and the editors Cawood and Kerr for their constructive criticisms of an earlier version of the manuscript.

#### References

- Altherr, R., Holl, A., Hegner, E., Langer, C., Kreuzer, H., 2000. High-potassium, calc-alkaline I-type plutonism in the European Variscides: northern Vosges (France) and northern Schwarzwald (Germany). *Lithos* 50, 51–73.
- Badarch, G., Dickson Cunningham, W., Windley, B.F., 2002. A new terrane subdivision for Mongolia: implications for the Phanerozoic crustal growth of Central Asia. *Journal of Asian Earth Sciences* 21, 87–110.
- Baker, P.E., 1968. Comparative volcanology and petrology of the Atlantic island-arcs. *Bulletin of Volcanology* 32, 189–206.
- Barth, A.P., Wooden, J.L., Jacobson, C.E., Economos, R.C., 2013. Detrital zircon as a proxy for tracking the magmatic arc system: The California arc example. *Geology* 41, 223–226.
- Berzin, N.A., Kungurtsev, L.V., 1996. Geodynamic interpretation of Altai–Sayan geological complexes. *Russian Geology and Geophysics* 37, 56–73.
- Berzin, N.A., Coleman, R.G., Dobretsov, N.L., Zonenshain, L.P., Xuchang, X., Chang, E.Z., 1994. Geodynamic map of the western part of the Paleozoic Ocean. *Russian Geology and Geophysics* 35, 5–22.
- Blichert-Toft, J., Albarède, F., 1997. The Lu–Hf isotope geochemistry of chondrites and the evolution of the mantle–crust system. *Earth and Planetary Science Letters* 148, 243–258.
- Buslov, M.M., 2011. Tectonics and geodynamics of the Central Asian Foldbelt: the role of Late Paleozoic large-amplitude strike-slip faults. *Russian Geology and Geophysics* 52, 52–71.
- Buslov, M.M., Safonova, I.Y., 2010. Siberian continent margins, Altai-Mongolian Gondwana-derived terrane and their separating suture–shear zone. Guide-book to the field excursion of the International workshop “Geodynamic evolution, tectonics and magmatism of the Central Asian Orogenic belt”.
- Buslov, M.M., Watanabe, T., 1996. Intrasubduction collision and its role in the evolution of an accretionary wedge: the Kurai zone of Gorny Altai (Central Asia). *Russian Geology and Geophysics of Geologia I Geofizika* 37, 74–84.
- Buslov, M.M., Saphonova, I.Yu., Watanabe, T., Obut, O.T., Fujiwara, Y., Iwata, K., Semakov, N.N., Sugai, Y., Smirnova, L.V., Kazansky, A.Yu., 2001. Evolution of the Paleo-Asian Ocean (Altai–Sayan Region, Central Asia) and collision of possible Gondwana-derived terranes with the southern marginal part of the Siberian continent. *Geosciences Journal* 5, 203–224.
- Buslov, M.M., Watanabe, T., Saphonova, I.Yu., Iwata, K., Travin, A., Akiyama, M., 2002. A Vendian–Cambrian Island Arc System of the Siberian Continent in Gorny Altai (Russia, Central Asia). *Gondwana Research* 5, 781–800.
- Buslov, M.M., Watanabe, T., Smirnova, L.V., Fujiwara, Y., Iwata, K., De Grave, J., Semakov, N.N., Travin, A.V., Kir’ynova, A.P., Kokh, D.A., 2003. Role of strike-slip faulting in Late Paleozoic–Early Mesozoic tectonics and geodynamics of the Altai–Sayan and East Kazakhstan regions. *Russian Geology and Geophysics* 44, 49–75.

- Buslov, M.M., Watanabe, T., Fujiwara, Y., Iwata, K., Smirnova, L.V., Safonova, I.Yu., Semakov, N.N., Kiryanova, A.P., 2004. Late Paleozoic faults of the Altai region, Central Asia: tectonic pattern and model of formation. *Journal of Asian Earth Sciences* 23, 655–671.
- Buslov, M.M., Geng, H., Travin, A.V., Otgonbaatar, D., Kulikova, A.V., Chen, M., Stijin, G., Semakov, N.N., Rubanova, E.S., Abildaeva, M.A., Voitishchik, E.E., Trofimova, D.A., 2013. Tectonics and geodynamics of Gorny Altai and adjacent structures of the Altai–Sayan folded area. *Russian Geology and Geophysics* 54, 1250–1271.
- Cai, K., Sun, M., Yuan, C., Zhao, G., Xiao, W., Long, X., Wu, F., 2010. Geochronological and geochemical study of mafic dykes from the northwest Chinese Altai: Implications for petrogenesis and tectonic evolution. *Gondwana Research* 18, 638–652.
- Cai, K., Sun, M., Yuan, C., Long, X., Xiao, W., 2011. Geological framework and Paleozoic tectonic history of the Chinese Altai, NW China: a review. *Russian Geology and Geophysics* 52, 1619–1633.
- Cai, K., Sun, M., Xiao, W., Buslov, M.M., Yuan, C., Zhao, G., Long, X., 2014. Zircon U–Pb geochronology and Hf isotopic composition of granitoids in Russian Altai Mountain, Central Asian Orogenic Belt. *American Journal of Science* 314, 580–612.
- Cawood, P.A., Hawkesworth, C.J., Dhuime, B., 2012. Detrital zircon record and tectonic setting. *Geology* 40, 875–878.
- Chappell, B.W., White, A.J.R., 2001. Two contrasting granite types: 25 years later. *Australian Journal of Earth Sciences* 48, 489–499.
- Charvet, J., Shu, L., Laurent-Charvet, S., 2007. Paleozoic structural and geodynamic evolution of eastern Tianshan (NW China): welding of the Tarim and Junggar plates. *Episodes* 30, 162–186.
- Chen, M., Sun, M., Cai, K., Buslov, M.M., Zhao, G., Rubanova, E.S., Voytishchik, E.E., 2014. Detrital zircon record of the early Paleozoic meta-sedimentary rocks in Russian Altai: Implications on their provenance and the tectonic nature of the Altai–Mongolian terrane. *Lithos* (<http://dx.doi.org/10.1016/j.lithos.2014.11.023>, in press).
- Cohen, K., Finney, S., Gibbard, P., Fan, J.-X., 2013. The ICS international chronostratigraphic chart. *Episodes* 36, 199–204.
- Corfu, F., Hanchar, J.M., Hoskin, P.W.O., Kinny, P., 2003. Atlas of zircon textures. *Reviews in Mineralogy and Geochemistry* 53, 469–500.
- De Grave, J., Buslov, M.M., Van Den Haute, P., Metcalf, J., Dehandschutter, B., McWilliams, M.O., 2009. Multi-method chronometry of the Teletskoye graben and its basement, Siberian Altai Mountains: new insights on its thermo-tectonic evolution. *Geological Society, London, Special Publications* 324, 237–259.
- Demoux, A., Kröner, A., Badarch, G., Jian, P., Tomurhuu, D., Wingate, M.T.D., 2009. Zircon Ages from the Baydrag Block and the Bayankhongor Ophiolite Zone: Time Constraints on Late Neoproterozoic to Cambrian Subduction- and Accretion-Related Magmatism in Central Mongolia. *The Journal of Geology* 117, 377–397.
- Dickinson, W.R., Gehrels, G.E., 2009. Use of U–Pb ages of detrital zircons to infer maximum depositional ages of strata: a test against a Colorado Plateau Mesozoic database. *Earth and Planetary Science Letters* 288, 115–125.
- Dobretsov, N.L., Buslov, M.M., 2004. Serpentinic Mélanges Associated with HP and UHP Rocks in Central Asia. *International Geology Review* 46, 957–980.
- Dobretsov, N.L., Buslov, M.M., 2007. Late Cambrian–Ordovician tectonics and geodynamics of Central Asia. *Russian Geology and Geophysics* 48, 71–82.
- Dobretsov, N.L., Berzin, N.A., Buslov, M.M., 1995. Opening and tectonic evolution of the Paleo-Asian Ocean. *International Geology Review* 37, 335–360.
- Dobretsov, N.L., Buslov, M.M., De Grave, J., Sklyarov, E.V., 2013. Interplay of magmatism, sedimentation, and collision processes in the Siberian craton and the flanking orogens. *Russian Geology and Geophysics* 54, 1135–1149.
- Gladkochub, D.P., Stanevich, A.M., Mazukabzov, A.M., Donskaya, T.V., Pisarevsky, S.A., Nicoll, G., Motova, Z.L., Kornilova, T.A., 2013. Early evolution of the Paleozoic ocean: LA-ICP-MS dating of detrital zircon from Late Precambrian sequences of the southern margin of the Siberian craton. *Russian Geology and Geophysics* 54, 1150–1163.
- Glorie, S., De Grave, J., Buslov, M.M., Zhimulev, F.I., Izmer, A., Vandoorne, W., Ryabinin, A., Van den haute, P., Vanhaecke, F., Elburg, M.A., 2011. Formation and Paleozoic evolution of the Gorny–Altai–Altai–Mongolia suture zone (South Siberia): Zircon U/Pb constraints on the igneous record. *Gondwana Research* 20, 465–484.
- Griffin, W.L., Pearson, N.J., Belousova, E., Jackson, S.E., Achterbergh, E., O'Reilly, S.Y., Shee, S.R., 2000. The Hf isotope composition of cratonic mantle: LAM-MC-ICPMS analysis of zircon megacrysts in kimberlites. *Geochimica et Cosmochimica Acta* 64, 133–147.
- Griffin, W.L., Wang, X., Jackson, S.E., Pearson, N.J., O'Reilly, S.Y., Xu, X., Zhou, X., 2002. Zircon chemistry and magma mixing, SE China: In-situ analysis of Hf isotopes, Tonglu and Pingtan igneous complexes. *Lithos* 61, 237–269.
- Hanchar, J.M., Miller, C.F., 1993. Zircon zonation patterns as revealed by cathodoluminescence and backscattered electron images: implications for interpretation of complex crustal histories. *Chemical Geology* 110, 1–13.
- Jahn, B.-M., 2004. The Central Asian Orogenic Belt and growth of the continental crust in the Phanerozoic. *Geological Society, London, Special Publications* 226, 73–100.
- Jahn, B., Wu, F., Chen, B., 2000. Massive granitoid generation in Central Asia: Nd isotope evidence and implication for continental growth in the Phanerozoic. *Episodes* 23, 82–92.
- Jahn, B., Wu, F., Chen, B., 2001a. Granitoids of the Central Asian Orogenic Belt and continental growth in the Phanerozoic. *Transactions Royal Society of Edinburgh* 91, 181–194.
- Jahn, B.-M., Wu, F.-Y., Chen, B., 2001b. Growth of Asia in the Phanerozoic–Nd Isotopic Evidence. *Gondwana Research* 4, 640–642.
- Jiang, Y., Sun, M., Zhao, G., Yuan, C., Xiao, W., Xia, X., Long, X., Wu, F., 2010. The ~390 Ma high-T metamorphic event in the Chinese Altai: A consequence of ridge-subduction? *American Journal of Science* 310, 1421–1452.
- Jiang, Y., Sun, M., Zhao, G., Yuan, C., Xiao, W., Xia, X., Long, X., Wu, F., 2011. Precambrian detrital zircons in the Early Paleozoic Chinese Altai: Their provenance and implications for the crustal growth of central Asia. *Precambrian Research* 189, 140–154.
- Jiang, Y., Sun, M., Kröner, A., Tumurkhuu, D., Long, X., Zhao, G., Yuan, C., Xiao, W., 2012. The high-grade Tsel Terrane in SW Mongolia: An Early Paleozoic arc system or a Precambrian siver? *Lithos* 142–143, 95–115.
- Jones, J.V., Connelly, J.N., Karlstrom, K.E., Williams, M.L., Doe, M.F., 2009. Age, provenance, and tectonic setting of Paleoproterozoic quartzite successions in the southwestern United States. *Geological Society of America Bulletin* 121, 247–264.
- Khain, E.V., Bibikova, E.V., Kröner, A., Zhuravlev, D.Z., Sklyarov, E.V., Fedotova, A.A., Kravchenko-Berezhnoy, I.R., 2002. The most ancient ophiolite of the Central Asian fold belt: U–Pb and Pb–Pb zircon ages for the Dunzhugur Complex, Eastern Sayan, Siberia, and geodynamic implications. *Earth and Planetary Science Letters* 199, 311–325.
- Khain, E.V., Bibikova, E.V., Salnikova, E.B., Kröner, A., Gibsher, A.S., Didenko, A.N., Degtyarev, K.E., Fedotova, A.A., 2003. The Palaeo-Asian ocean in the Neoproterozoic and early Palaeozoic: new geochronologic data and palaeotectonic reconstructions. *Precambrian Research* 122, 329–358.
- Kovalenko, V.I., Yarmolyuk, V.V., Kovach, V.P., Kotov, A.B., Kozakov, I.K., Salnikova, E.B., Larin, A.M., 2004. Isotope provinces, mechanisms of generation and sources of the continental crust in the Central Asian mobile belt: geological and isotopic evidence. *Journal of Asian Earth Sciences* 23, 605–627.
- Kröner, A., Kovach, V., Belousova, E., Hegner, E., Armstrong, R., Dolgoplova, A., Seltmann, R., Alexeev, D.V., Hoffmann, J.E., Wong, J., Sun, M., Cai, K., Wang, T., Tong, Y., Wilde, S.A., Degtyarev, K.E., Rytsh, E., 2014. Reassessment of continental growth during the accretionary history of the Central Asian Orogenic Belt. *Gondwana Research* 25, 103–125.
- Kruk, N.N., Rudnev, S.N., Shokalsky, S.P., Babin, G.A., Kuibida, M.L., Lepekina, E.N., Kovach, V.P., 2007. Age and tectonic position of plagiogranites of Sarakoksha massive (Altai Mountains). *Litosfera* 6, 137–146 (in Russian).
- Kruk, N.N., Vladimirov, A.G., Babin, G.A., Shokalsky, S.P., Sennikov, N.V., Rudnev, S.N., Volkova, N.I., Kovach, V.P., Serov, P.A., 2010. Continental crust in Gorny Altai: nature and composition of protoliths. *Russian Geology and Geophysics* 51, 431–446.
- Kruk, N.N., Rudnev, S.N., Vladimirov, A.G., Shokalsky, S.P., Kovach, V.P., Serov, P.A., Volkova, N.I., 2011. Early–Middle Paleozoic granitoids in Gorny Altai, Russia: Implications for continental crust history and magma sources. *Journal of Asian Earth Sciences* 42, 928–948.
- Liu, Y., Gao, S., Hu, Z., Gao, C., Zong, K., Wang, D., 2010. Continental and Oceanic Crust Recycling-induced Melt–Peridotite Interactions in the Trans-North China Orogen: U–Pb Dating, Hf Isotopes and Trace Elements in Zircons from Mantle Xenoliths. *Journal of Petrology* 51, 537–571.
- Long, X., Sun, M., Yuan, C., Xiao, W., Lin, S., Wu, F., Xia, X., Cai, K., 2007. Detrital zircon age and Hf isotopic studies for metasedimentary rocks from the Chinese Altai: Implications for the Early Paleozoic tectonic evolution of the Central Asian Orogenic Belt. *Tectonics* 26, TC5015.
- Long, X., Yuan, C., Sun, M., Xiao, W., Zhao, G., Wang, Y., Cai, K., Xia, X., Xie, L., 2010. Detrital zircon ages and Hf isotopes of the early Paleozoic flysch sequence in the Chinese Altai, NW China: New constraints on depositional age, provenance and tectonic evolution. *Tectonophysics* 480, 213–231.
- Ludwig, K.R., 2003. *Isoplot/Ex Version 3.00, a Geochronological Toolkit for Microsoft Excel*. Berkeley Geochronology Center, Berkeley, CA, USA.
- Machado, N., 2001. U–Pb dating and Hf isotopic composition of zircon by laser ablation MC-ICP-MS. *Laser ablation-ICPMS in the Earth sciences: Principles and applications*.
- Ota, T., Buslov, M.M., Watanabe, T., 2002. Metamorphic Evolution of Late Precambrian Eclogites and Associated Metabasites, Gorny Altai, Southern Russia. *International Geology Review* 44, 837–858.
- Ota, T., Utsunomiya, A., Uchio, Y., Isozaki, Y., Buslov, M.M., Ishikawa, A., Maruyama, S., Kitajima, K., Kaneko, Y., Yamamoto, H., Katayama, I., 2007. Geology of the Gorny Altai subduction–accretion complex, southern Siberia: Tectonic evolution of an Ediacaran–Cambrian intra-oceanic arc–trench system. *Journal of Asian Earth Sciences* 30, 666–695.
- Petrulina, Z.E., Sennikov, N.V., Ermikov, V.D., 1984. Stratigraphy of the Lower Ordovician of Gorny Altai. *Stratigraphy and Fauna of the Lower Ordovician of Gorny Altaipp*. 3–33.
- Ponomarchuk, V.A., Travin, A.V., Simonov, V.A., Palessky, S.V., Kuzmin, D.S., Stupakov, S.I., 1993. The initial Argon composition of the Altay Mountains and Mongolian ophiolites. *Geodynamic evolution of Paleozoic ocean: Novosibirsk, IUGG, Report No. 4 of the IGCP Project* 283.
- Rosen, O.M., Condie, K.C., Natapov, L.M., Nozhkin, A.D., 1994. Archean and early Proterozoic evolution of the Siberian craton: a preliminary assessment. In: Condie, K.C. (Ed.), *Archean Crustal Evolution*. Elsevier, Amsterdam, pp. 411–459.
- Rudnev, S.N., Borisov, S.M., Babin, G.A., Levchenko, O.A., Makeev, A.F., Serov, P.A., Matukov, D.I., Plotkina, Yu.V., 2008. Early Paleozoic batholiths in the northern part of the Kuznetsk Alatau: Composition, age, and sources. *Petrology* 16, 395–419.
- Rudnev, S.N., Babin, G.A., Kovach, V.P., Kiseleva, V.Y., Serov, P.A., 2013. The early stages of island-arc plagiogranitoid magmatism in Gornaya Shoriya and West Sayan. *Russian Geology and Geophysics* 54, 20–33.
- Safonova, I., 2008. Geochemical evolution of intraplate magmatism in the Paleo-Asian Ocean from the Late Neoproterozoic to the Early Cambrian. *Petrology* 16, 492–511.
- Safonova, I.Y., Buslov, M.M., Iwata, K., Kokh, D.A., 2004. Fragments of Vendian–Early Carboniferous Oceanic Crust of the Paleo-Asian Ocean in Foldbelts of the Altai–Sayan Region of Central Asia: Geochemistry, Biostratigraphy and Structural Setting. *Gondwana Research* 7, 771–790.
- Safonova, I., Maruyama, S., Hirata, T., Kon, Y., Rino, S., 2010. LA ICP MS U–Pb ages of detrital zircons from Russia largest rivers: implications for major granitoid events in Eurasia and global episodes of supercontinent formation. *Journal of Geodynamics* 50, 134–153.
- Safonova, I.Y., Buslov, M.M., Simonov, V.A., Izokh, A.E., Komiya, T., Kurganskaya, E.V., Ohno, T., 2011. Geochemistry, petrogenesis and geodynamic origin of basalts from

- the Katun' accretionary complex of Gorny Altai (southwestern Siberia). *Russian Geology and Geophysics* 52, 421–422.
- Scherer, E., Münker, C., Mezger, K., 2001. Calibration of the Lutetium–Hafnium Clock. *Science* 293, 683–687.
- Sengör, A.M.C., Natal'in, B.A., Burtman, V.S., 1993. Evolution of the Altaid tectonic collage and Palaeozoic crustal growth in Eurasia. *Nature* 364, 299–307.
- Simonov, V.A., Dobretsov, N.L., Buslov, M.M., 1994. Boninite series in structures of the Paleo-Asian ocean. *Geology and Geophysics* 35, 172–189.
- Sun, M., Yuan, C., Xiao, W., Long, X., Xia, X., Zhao, G., Lin, S., Wu, F., Kröner, A., 2008. Zircon U–Pb and Hf isotopic study of gneissic rocks from the Chinese Altai: Progressive accretionary history in the early to middle Palaeozoic. *Chemical Geology* 247, 352–383.
- Terleev, A.A., 1991. Stratigraphy of Vendian–Cambrian sediments of the Katun anticline (Gorny Altai). In: Khomentovskiy, V.V. (Ed.), *Late Precambrian and Early Paleozoic of Siberia*. IJGGM Publishing, Novosibirsk, pp. 82–106 (in Russian).
- Uchio, Y., Isozaki, Y., Nohda, S., Kawahara, H., Ota, T., Buslov, M.M., Maruyama, S., 2001. The Vendian to Cambrian paleo-environment in shallow mid-ocean: stratigraphy of Vendo-Cambrian seamount-top limestone in the Gorny Altai mountains, southern Russia. Program and late abstracts for UNESCO-IUGS-IGCP 368/411/440 International Symposium on the Assembly and Breakup of Rodinia and Gondwana, and Growth of Asia. Osaka, Japan. GRG/GIGE Miscellaneous Publication 12, pp. 47–48.
- Uchio, Y., Isozaki, Y., Ota, T., Utsunomiya, A., Buslov, M.M., Maruyama, S., 2004. The oldest mid-oceanic carbonate buildup complex: Setting and lithofacies of the Vendian (Late Neoproterozoic) Baratal limestone in the Gorny Altai Mountains, Siberia. *Proceedings of the Japan Academy Series B* 9, 422–428.
- Vernikovskiy, V.A., Vernikovskaya, A.E., Kotov, A.B., Sal'nikova, E.B., Kovach, V.P., 2003. Neoproterozoic accretionary and collisional events on the western margin of the Siberian craton: new geological and geochronological evidence from the Yenisey Ridge. *Tectonophysics* 375, 147–168.
- Wang, B., Chen, Y., Zhan, S., Shu, L., Faure, M., Cluzel, D., Charvet, J., Laurent-Charvet, S., 2007. Primary Carboniferous and Permian paleomagnetic results from the Yili Block (NW China) and their implications on the geodynamic evolution of Chinese Tianshan Belt. *Earth and Planetary Science Letters* 263, 288–308.
- Wang, C.Y., Campbell, I.H., Stepanov, A.S., Allen, C.M., Burtsev, I.N., 2011. Growth rate of the preserved continental crust: II. Constraints from Hf and O isotopes in detrital zircons from Greater Russian Rivers. *Geochimica et Cosmochimica Acta* 75, 1308–1345.
- Wang, Y., Long, X., Wilde, S.A., Xu, H., Sun, M., Xiao, W., Yuan, C., Cai, K., 2014. Provenance of Early Paleozoic metasediments in the central Chinese Altai: Implications for tectonic affinity of the Altai–Mongolia terrane in the Central Asian Orogenic Belt. *Lithos* 210–211, 57–68.
- Wiedenbeck, M., Alle, P., Corfu, F., Griffin, W.L., Meier, M., Oberli, F., Quadt, A., Roddick, J.C., Spiegel, W., 1995. Three natural zircon standards for U–Th–Pb, Lu–Hf, trace element and REE analyses. *Geostandards and Geoanalytical Research* 19, 1–23.
- Wilhelm, C., Windley, B.F., Stampfli, G.M., 2012. The Altaids of Central Asia: A tectonic and evolutionary innovative review. *Earth-Science Reviews* 113, 303–341.
- Windley, B.F., Alexeiev, D., Xiao, W., Kröner, A., Badarch, G., 2007. Tectonic models for accretion of the Central Asian Orogenic Belt. *Journal of the Geological Society* 164, 3–47.
- Wu, F.-Y., Jahn, B.-M., Wilde, S., Sun, D.-Y., 2000. Phanerozoic crustal growth: U–Pb and Sr–Nd isotopic evidence from the granites in northeastern China. *Tectonophysics* 328, 89–113.
- Wu, F.-Y., Ji, W.-Q., Liu, C.-Z., Chung, S.-L., 2010. Detrital zircon U–Pb and Hf isotopic data from the Xigaze fore-arc basin: Constraints on Transhimalayan magmatic evolution in southern Tibet. *Chemical Geology* 271, 13–25.
- Xia, X., Sun, M., Geng, H., Sun, Y., Wang, Y., Zhao, G., 2011. Quasi-simultaneous determination of U–Pb and Hf isotope compositions of zircon by excimer laser-ablation multiple-collector ICPMS. *Journal of Analytical Atomic Spectrometry* 26, 1868–1871.
- Xiao, W., Windley, B.F., Hao, J., Zhai, M., 2003. Accretion leading to collision and the Permian Solonker suture, Inner Mongolia, China: Termination of the central Asian orogenic belt. *Tectonics* 22, 1069.
- Xiao, W.-J., Zhang, L.-C., Qin, K.-Z., Sun, S., Li, J.-L., 2004. Paleozoic accretionary and collisional tectonics of the eastern Tianshan (China): Implications for the continental growth of central Asia. *American Journal of Science* 304, 370–395.
- Xiao, W.J., Windley, B.F., Huang, B.C., Han, C.M., Yuan, C., Chen, H.L., Sun, M., Sun, S., Li, J.L., 2009a. End-Permian to mid-Triassic termination of the accretionary processes of the southern Altaids: implications for the geodynamic evolution, Phanerozoic continental growth, and metallogeny of Central Asia. *International Journal of Earth Sciences* 98, 1189–1217.
- Xiao, W.J., Windley, B.F., Yuan, C., Sun, M., Han, C.M., Lin, S.F., Chen, H.L., Yan, Q.R., Liu, D.Y., Qin, K.Z., Li, J.L., Sun, S., 2009b. Paleozoic multiple subduction–accretion processes of the southern Altaids. *American Journal of Science* 309, 221–270.
- Xiao, W., Huang, B., Han, C., Sun, S., Li, J., 2010. A review of the western part of the Altaids: A key to understanding the architecture of accretionary orogens. *Gondwana Research* 18, 253–273.
- Yang, T.N., Li, J.Y., Zhang, J., Hou, K.J., 2011. The Altai–Mongolia terrane in the Central Asian Orogenic Belt (CAOB): A peri-Gondwana one? Evidence from zircon U–Pb, Hf isotopes and REE abundance. *Precambrian Research* 187, 79–98.
- Yolkina, E.A., Sennikov, N.V., Buslov, M.M., Yazikov, A., 1994. Paleogeographic reconstructions of the western Altai–Sayan Region in the Ordovician, Silurian and Devonian and their geodynamic implications. *Russian Geology and Geophysics* 35, 100–125.
- Yuan, C., Sun, M., Xiao, W., Li, X., Chen, H., Lin, S., Xiao, X., Long, X., 2007. Accretionary orogenesis of the Chinese Altai: Insights from Paleozoic granitoids. *Chemical Geology* 242, 22–39.
- Zonenshain, L.P., Kuzmin, M.I., Natapov, L.M., 1990. *Geology of the USSR: a plate-tectonic synthesis*. American Geophysical Union Geodynamics Series 21.